

EFFECTS OF HYDROGEL NANOPARTICLES AS A NOVEL ADJUVANT FOR A
PURIFIED WHOLE INACTIVATED CHIKUNGUNYA VIRUS VACCINE

by

Kassandra Jackson
A Thesis
Submitted to the
Graduate Faculty
of
George Mason University
in Partial Fulfillment of
The Requirements for the Degree
of
Master of Science
Biology

Committee:

_____ Dr. Alessandra Luchini, Thesis Director

_____ Dr. Lance Liotta, Committee Member

_____ Dr. Kylene Kehn-Hall, Committee Member

_____ Dr. Iosif Vaisman, Acting Director, School
of Systems Biology

_____ Dr. Donna Fox, Associate Dean,
Office of Student Affairs & Special
Programs, College of Science

_____ Dr. Peggy Agouris, Dean, College of Science

Date: _____ Fall Semester 2016
George Mason University
Fairfax, VA

Effects of Hydrogel Nanoparticles as a Novel Adjuvant for a Purified Whole Inactivated
Chikungunya Virus Vaccine

A Thesis submitted in partial fulfillment of the requirements for the degree of Master of
Science at George Mason University

by

Kassandra Jackson
Bachelor of Arts
George Mason University, 2016

Director: Alessandra Luchini, Associate Professor
Department of Biology

Fall Semester 2016
George Mason University
Fairfax, VA



This work is licensed under a [creative commons attribution-noncommercial 3.0 unported license](https://creativecommons.org/licenses/by-nc/3.0/).

DEDICATION

This is dedicated to my darling Daniel, the light at the end of this tunnel. I will meet you in paradise.

ACKNOWLEDGEMENTS

I would like to thank the many friends, relatives, and supporters who have made this happen. My loving fiancé, Dan, helping me set goals and with my revisions. My colleague, Rafael, assisting me in my research. Finally, thanks go out to Drs. Luchini, Liotta, and the other members of my committee for their invaluable help.

TABLE OF CONTENTS

	Page
List of Tables	vii
List of Figures	viii
List of Abbreviations	ix
Abstract	x
Chapter One: Background.....	1
1.0: Introduction to Chikungunya Virus.....	1
1.1: Geographical Distribution	5
1.2: Transmission.....	6
1.3: Current vaccines and treatments.....	7
2.0: History of Adjuvants	9
2.1: Aluminum Adjuvant.....	10
2.2: Other Types of Adjuvants	12
3.0: Nanoparticle vaccine delivery vehicles.....	14
3.1: Hydrogel Nanotrap Nanoparticle	16
Chapter Two: Production and validation of hydrogel nanotrap nanoparticles to capture Chikungunya	19
1.0: Introduction	19
2.0 Methods	20
2.1: Production of nanoparticles	20
2.2: Validate nanoparticles with purified inactivated CHIKV through Plaque Assay	22
2.3: Size characterization of nanoparticle.....	24
2.4: Time-release study of CHIKV with selected nanoparticles	24
3.0 Results	27
3.1: Nanoparticles captured CHIK virus	27
3.2: Size characterization of nanoparticle before and after autoclaving.....	30

3.3: Autoclaved nanoparticles are able to capture virus	33
3.4: The selected nanoparticle is adsorbed to vaccine and is not released	36
4.0 Discussion	38
Chapter Three: Investigation of the immune response of selected hydrogel nanotrap nanoparticles as a novel adjuvant for a chikungunya virus vaccine by mouse trials.....	42
1.0 Introduction	42
2.0 Methods	46
2.1: mouse study and neutralization antibody assay	46
2.2: Optimization of Cell-mediated immunity test.....	48
3.0 Results	50
3.1 Nanoparticle adjuvant matched the immunogenicity of the non-adjuvanted vaccine	50
3.2 Determine the cell-mediated immunity from the mouse spleens.	54
4.0 Discussion	55
Chapter Four: Determination of the level of toxicity of the hydrogel nanotrap nanoparticles in mouse model.....	59
1.0 Introduction	59
2.0 Methods	63
2.1: Toxicity examination on mice used in study.....	63
3.0 Results	63
3.1: No signs of toxicity.	63
4.0 Discussion	67
References.....	71

LIST OF TABLES

Table	Page
Table 1 Initial mouse toxicity examination	64

LIST OF FIGURES

Figure	Page
Figure 1 96-well ELISA plate layout.....	26
Figure 2 Nanoparticle screening with CHIKV Results.....	Error! Bookmark not defined.
Figure 3 NanoSight Characterization of non-autoclaved and autoclaved NP	Error! Bookmark not defined.
Figure 4 Plaque assay results of the autoclaved nanoparticles.	Error! Bookmark not defined.
Figure 5 Time-release study.....	Error! Bookmark not defined.
Figure 6 96-well plate layout for the micro neutralization	47
Figure 7 Neutralizing geometric mean titers and Seropositive Rate for neutralization....	54
Figure 8 Tissue toxicity examination.....	66

LIST OF ABBREVIATIONS

Nanoparticles	NPs
Chikungunya Virus	CHIKV
50% Tissue culture Infective Dose	TCID ₅₀
East Central and South African.....	ECSA
Ribonucleic acid	RNA
United Kingdom.....	UK
Deoxyribonucleic acid	DNA
Natural killer cell	NK
U.S. Center for Disease Control and Prevention	CDC
US Army Medical Research Institute of Infectious Disease	USAMRIID
Virus-like particle	VLP
Damage-associated molecular patterns.....	DAMPs
Dendritic cells	DCs
Antigen presenting cell	APC
Toll-like receptor	TLR
Monophosphoryl lipid A	MPL
lipopolysaccharide	LPS
Major histocompatibility complex.....	MHC
poly(N-isopropylacrylamide).....	pNIPAm
methylenebisacrylamide	BIS
Reverse Osmosis/Deionized	RODI
World Health Organization.....	WHO
Disperse Yellow 3	DY3
Purified inactivated virus	PIV
Remazol Brilliant Blue R.....	RBB
Enzyme Linked Immunosorbent Assay	ELISA
Phosphate Buffer Saline.....	PBS
Horseradish Peroxidase.....	HRP
Plaque Forming Unit.....	PFU
ELISA Unit.....	EU

ABSTRACT

EFFECTS OF HYDROGEL NANOPARTICLES AS A NOVEL ADJUVANT FOR A PURIFIED WHOLE INACTIVATED CHIKUNGUNYA VIRUS VACCINE

Kassandra Jackson,

George Mason University, 2016

Thesis Director: Dr. Alessandra Luchini

This thesis describes a novel nanotrap nanoparticle adjuvant for a purified whole inactivated Chikungunya CHIK virus vaccine and its immune response and level of toxicity. For a vaccine to be good candidate it must be able to invoke a strong immune response to the viral antigen without causing damage to the recipient. Most vaccines are formulated with an adjuvant, which is anything that has the ability to bolster the immune response to the vaccine. Nanoparticle pose as a promising alternative to the commonly used alum adjuvant. The novel chemistry of the nanoparticles used in this study allows them to deliver the drug to the desired area, gradually release their cargo, and stabilize and protect the vaccine. Following a 28-day mouse trail, blood sera from the placebo group, non-adjuvanted CHIK vaccine group and NP-adjuvanted CHIK vaccine group were tested for neutralizing antibodies. Each vaccine group was also tested for signs of toxicity. The neutralizing titers from the NP-adjuvanted vaccine group was substantially

equivalent to the non-adjuanted vaccine group. Moreover, the author showed that the NPs were able to capture whole CHIK virus, remain adsorbed to the virus for an extended period of time and that the NPs were non-toxic.

CHAPTER ONE: BACKGROUND

Before the early 2000s the mosquito-transmitted disease, Chikungunya Virus, was mainly found in tropical and subtropical areas of Africa and of South and Southeast Asia. Outbreaks were small and rare and transmission was predominately through the mosquito endemic to those regions. Since the early 2000s Chikungunya virus has evolved to cause outbreaks in North America and Europe. There is currently no vaccine for the virus or treatment for the disease. As more and more outbreaks appear in parts of the world that, in the past, never encountered this virus, the need for a vaccine becomes more urgent especially now that the virus is no longer restricted to developing tropical countries. The threat of an epidemic in the United States becomes a very real possibility.

1.0: Introduction to Chikungunya Virus

CHIKV is part of the genus *Alphavirus* and belongs to the *Togaviridae* family. The family *Togaviridae* is made up of two genera, *Alphavirus* and *Rubivirus*. Most viruses in the *Alphavirus* genus are typically maintained in natural cycles involving transmission by an arthropod vector to a vertebrate host. Many of the Old World *Alphavirus* viruses cause similar symptoms, such as arthralgia. *Alphavirus* viruses, including CHIKV, consist of a linear positive-sense single-stranded RNA genome¹. CHIKV's genome is roughly 12 kb encoding non-structural proteins (nsP1-nsP4), three structural proteins (C, E1, and E2), and two proteins of unknown function (E3 and 6K)^{2,3}.

Viral entry for CHIKV occurs through a pH-dependent, endocytic pathway, most likely a clathrin mediated pathway⁴. Studies have shown that viral replication can be blocked by compounds inhibiting endosomal acidification, supporting the supposed method for entry⁴.

Like many *Alphavirus* viruses, replication occurs in the cytoplasm. Following endocytosis, a conformational change occurs that exposes the E1 peptide. This allows the delivery of the core and release of the viral genome into the cytoplasm⁵. Two precursors of non-structural proteins (nsPs) are translated from the viral mRNA, and cleavage of these precursors generates nsP1–nsP4. nsP1⁵. During viral replication, nsP1 is thought to catalyze the start of the negative-strand RNA synthesis. This process is supported by the nsP4 that possesses a RNA-dependent polymerase motif⁶. The nsP1 is also part of the capping and methylation of the positive-strand RNA. The nsP3 is able to bind to RNA and plays a role in transcribing the negative strand by facilitating the recruitment of RNA by other non-structural proteins⁵. The nsP2 protein has both helicase and proteinase abilities and help cleave the nsP123 polyprotein⁵. These proteins assemble to form the viral replication complex, which synthesizes a full-length negative-strand RNA intermediate. This serves as the template for the synthesis of both subgenomic (26S) and genomic (49S) RNAs. The subgenomic RNA drives the expression of the C–pE2–6K–E1 polyprotein precursor⁵. The capsid (C) is released, and the pE2 and E1 glycoproteins are generated by further processing. pE2 and E1 associate in the Golgi and are exported to the plasma membrane, where pE2 is cleaved into E2 and E3^{5–7}. The capsid protein is mainly involved in the assembly of the viral nucleocapsid core. The E1 and E2 proteins

form heterodimers that arrange as trimeric spikes on the viral surface. E2 is on top of the spike and interacting with cell receptors and E1 generally facilitates viral entry through fusion of viral and plasma membranes⁵⁻⁷. Viral assembly is promoted by binding of the viral nucleocapsid to the viral RNA and the recruitment of the membrane-associated envelope glycoproteins. The assembled alphavirus particle, with an icosahedral core, buds at the cell membrane.⁵

CHIKV replicates in various human adherent cells, including epithelial and endothelial cells, and primary fibroblasts and macrophages. The life cycle of this virus is short: as soon as 8–16 hours post infection numerous newly infected cells can be detected, which release high levels of progeny virions. Viral titers in supernatants reach 10^5 – 10^8 TCID₅₀/ml, depending on the cell type⁴. CHIKV is highly cytopathic in human cell cultures, and infected cells rapidly undergo apoptosis. The release of apoptotic blebs from dying cells has been shown to increase the spread of CHIKV from apoptotic-infected cells to uninfected neighboring cells as well as macrophages. Uninfected macrophages are then infected following phagocytosis of CHIKV-containing blebs, thus apoptosis potentially acts as a way for CHIKV to infect cells that are non-permissive to direct viral entry^{4,8,9}.

In Swahili and Makonde, the term “chikungunya” means “the bent walker” or “that which bends up” describing the main symptoms of the disease. CHIKV is characterized by rapid onset of fever and joint pain. The incubation period is 1 to 12 days, symptoms generally starting 4–7 d after the bite. Acute infection lasts 1–10 d and is characterized by a painful polyarthralgia, high fever, asthenia, headache, vomiting, rash,

and myalgia⁴. The joint pain is often very debilitating, but usually lasts for a few days or may be prolonged to weeks. In numerous patients, a chronic and incapacitating arthralgia persists for months. In severe cases, symptoms can last for several years. Asymptomatic infections are rare but occur in about 3-25% of people with serological evidence of the infection but have no obvious symptoms^{4,9,10}. Polyarthralgia is one of the most common symptom of CHIKV fever and also the most debilitating symptom. Nearly all patients with CHIKV infection have arthralgia that affects the body symmetrically and usually in multiple joints¹⁰. Fingers, wrists, ankles, elbows, toes, and knees are the most often affected. Patients with joints already damaged from other underlying disorders such as osteoarthritis are more susceptible. Most people infected will see improvement in their arthralgia 1-2 weeks after acute onset of disease. By that point, some recover fully, but many will continue to have persistent arthralgia that can last up to a year¹⁰.

Many factors increase the likelihood of persistent arthralgia such as age, underlying disorders, and severity of pain at disease onset. Children are also at high risk for severe symptoms such as abrupt onset high-grade fever, skin rashes, and swollen ankles or wrists^{10,11}. The chronic arthralgia phase, which occurs in about 50% of infected patients, is normally characterized by relapses and pain of varying intensities, usually affecting the same sites that were affected at the onset of the disease. Generally the chronic phase is not as severe as the acute phase, but people still substantial loose movement and quality of life.

Until recently CHIKV was not thought to be a neurotropic virus. But since the La Reunion outbreak much evidence shows a neurological involvement in CHIKV infection.

Some of the neurological complications include encephalopathy, encephalitis, acute flaccid paralysis, Guillian Barre syndrome, and febrile seizures^{10,11}. The La Reunion outbreak was also the first case of vertical transfer of the virus from mother to child. Since the 2006 La Reunion outbreaks the case fatality rate is about 1 in 1000¹⁰.

1.1: Geographical Distribution

Chikungunya is suspected to have been circulating enzootically in Africa for centuries. The first suspected outbreak occurred in the 18th century in Indonesia, where it was thought to have transferred from Africa on sailing ships. At that time there were many reports of epidemics in the West Indies and India, mainly Calcutta, with the symptoms consistent with CHIKV^{7,12}. It was not until 1952, in the Makonde Plateau in Tanzania, that the first outbreak of chikungunya fever was confirmed and first isolated. In Asia the virus was first isolated in 1958 in Bangkok. India's first confirmed epidemic of CHIKV was in 1963. Between the 1960s and 2000s, evidence of CHIKV occurred in numerous countries in western Africa as well in central and southern Africa. During this period, sporadic outbreaks occurred in south Asia and Southeast Asia¹².

Between 2005- 2007 a large outbreak of CHIKV occurred in the La Reunion, a small island in the Indian Ocean. During that outbreak 2,440,000 cases were reported and 203 deaths were associated with the infection¹⁰. From 2004-2007 new geographical areas started to report cases of CHIKV. Cases were reported in Europe (UK, Belgium, Germany, Czech Republic, Norway, Italy, Spain, and France), Hong Kong, Canada, Taiwan, Sri Lanka, and the USA¹³. In 2013, CHIKV appeared in Saint Martin and spread through the French West Indies, other Caribbean Islands and onto Central and South

Americas. In 2014, the Pan American Health Organization recorded more than 355,000 potential cases of chikungunya fever and the CDC reported 232 imported cases¹⁴. As of May 22, 2016 the U.S. Center for Disease Control and Prevention CDC reported a total of approximately 1.7 million suspected and 14,000 confirmed cases of CHIKV in 45 countries or territories in the Caribbean, Central America, South America and North America.

1.2: Transmission

CHIKV is mainly distributed throughout Africa, India and South East Asia. Currently, there are three lineages of CHIKV that are believed to be circulating- a West African lineage, an East Central and South African (ECSA) lineage, and a Asian lineage³. In Asia, Chikungunya is predominantly transmitted in a mosquito-human-mosquito cycle by *Aedes aegypti*^{2,3}, While in Africa, the virus is believed to be distributed through a sylvatic cycle that involves wild, non-human primates and a forest-dwelling *Aedes* mosquitos species^{2,3,15}. But in Africa, the virus has spilled over to the urban setting by transmission through domestic *A. aegypti*.

Studies of isolates from the severe 2005-2006 La Reunion outbreak showed a novel clade of the ECSA genotype containing a minor mutation. This mutation allowed the increased spread of CHIKV and a more severe form of the disease in terms of human symptoms^{2,3,7,14,16}. The mutation also allowed the chikungunya virus to be more transmissible by the *A. albopictus* mosquito, a mosquito susceptible to CHIKV infection but an atypical vector for human transmission¹⁶. Analysis of the mutation from the La Reunion outbreak epidemic identified a change of the alanine to valine of amino acid 226

of the E1 protein (E1-226V)^{3,16}. Studies suggest this single mutation is responsible for the enhanced infectivity in both *A. albopictus* and *A. aegypti* mosquitos. This change also reduced the cholesterol dependence and helped in replication and transmission of the virus^{3,16}. The La Reunion CHIKV outbreak, the abundance and distribution of *A. albopictus* mosquitos in Europe and the United States, and the identification of the E1-226V mutation showed that this disease was no longer restricted to third world countries^{7,16}.

1.3: Current vaccines and treatments

The only recommended treatment for CHIKV-induced arthralgia are non-steroidal ant-inflammatory drugs. Some possible treatments are CHIKV antibodies and chloroquine¹⁰. Mouse models have shown that the transfer of CHIKV immune serum protects against CHIKV induced lethality, suggesting that monoclonal antibodies could be a possible prophylactic treatment or provide protection immediately after being infected¹⁰.

Several prospects for a CHIKV vaccine are currently in the developmental or clinical stages. These include inactivated whole virus vaccines, live attenuated vaccines, virus-like particle (VLP) vaccines, and DNA vaccines^{2,12}. One vaccine developed at the US Army Medical Research Institute of Infectious Disease (USAMRIID), a live-attenuated CHIKV vaccine strain 181/25, was tested in humans and showed to be immunogenic in phase I and phase II clinical trials. Although the results showed this to be a promising candidate, about 8% of vaccines showed transient mild arthralgia^{2,12,17}. According to Gorchakov et al., there were only two amino acid substitutions in the E2

envelope glycoprotein that were responsible for attenuation of the wild type strain AF15561. These substitutions made the derived live attenuated strain 181/25 genetically unstable^{12,17}. In addition to the USAMRIID live-attenuated vaccine, several DNA vaccines have been designed. One DNA vaccine created for CHIKV expressed the capsid protein; another DNA vaccine was designed to express the envelope proteins. The capsid expressing DNA vaccine was not able to protect the mice in trials, but the envelope expressing DNA vaccine induced neutralizing antibodies after three biweekly doses¹². Another vaccine candidate for CHIKV, VLP-based vaccine expressing the E1, E2 and E3 proteins, has shown good promise in animal trials and clinical trials. In a non-human primate study, the vaccine showed high titers of neutralizing antibodies after three doses and protected the monkeys after challenge¹². The vaccine has completed a phase 1 clinical trial in healthy adults and the VLP-vaccine was shown to be immunogenic, safe and tolerated well after three doses¹⁸.

In an attempt to increase the safety of attenuated vaccine viruses, one group deleted a large portion of the nsP3 gene. Vaccine preparations consisted of the mutated viruses produced as viral particles or DNA-launched infectious genomes. Mice that received a single vaccination of either mutant vaccine had high levels of neutralizing antibody, a strong T cell response, and were protected against high-dose virus challenge. A second dose of the vaccine increased immunogenicity⁸.

An alternative to live attenuated vaccine candidates has been chimera alphavirus vaccines candidates. They have the backbone of other attenuated alphaviruses and contain the structural proteins of a CHIKV strain. The vaccine candidate showed to

produce a strong humoral immune response and did not trigger reactogenicity in adult mouse studies³.

In the absence of a vaccine, controlling the spread of chikungunya is primarily centered on vector control. Strategies to reduce potential breeding sites, killing larvae through larvicides and reducing the number of adult mosquitoes by spraying areas with pyrethroids or organophosphates are critical for preventing the further spread of CHIKV³.

2.0: History of Adjuvants

The concept of adjuvants started around the mid 1920s, when Gaston Ramon discovered that adding substances such as bread crust or tapioca to diphtheria toxoid in a vaccine formulation increased immune responses against the toxoid¹⁹. The following year, Alexander Glenny administered a diphtheria toxoid that was formulated with potassium aluminum sulfate (alum) that reported a better immune response compared to the antigen alone¹⁹.

The use of adjuvants in vaccine formulation is a commonly used method to increase the immunogenicity of a vaccine and to reduce the number of booster doses for a vaccine. Adjuvants can be molecules, compounds, or macromolecules that boost the potency and longevity of specific immune response to antigen, but cause minimal toxicity and have no immune effects themselves²⁰. One of the major appeals to the addition of adjuvants to vaccines is that it reduces the amount of antigen or number of immunizations required. They can also improve the efficacy of vaccines in newborns, elderly or immune-compromised individuals²⁰. Effective adjuvants utilize multiple mechanisms to

achieve a strong immunological response such as; long lasting antigen deposits, increased vaccine - antigen presentation by dendritic cells and the induction of CD4 T helper cells.

There are two classes of adjuvants commonly found in most vaccines today; immunostimulants that can act directly on the immune system to increase the response to antigens and vehicles that present vaccine antigens to the immune system in an optimal way²⁰. Vehicle adjuvants can control the release of the vaccine or be a depot delivery system, they can also deliver the antigen to a targeted area. Adjuvants need to be safe, stable prior to administration, easily biodegraded and eliminated, able to promote and antigen specific response and inexpensive to manufacture.

2.1: Aluminum Adjuvant

Alum remains the primary adjuvant in general use for vaccines since its discovered use in 1926, where incorporating aluminum sulfate salts (alum) in a vaccine enhanced the vaccine's immune response. Aluminum hydroxide and aluminum phosphate adjuvants are generally prepared by exposing aqueous solutions of aluminum ions to alkaline conditions under very controlled circumstances, which in the case of aluminum phosphate takes place in the presence of phosphate ions¹⁹. Various soluble aluminum salts can be used for the production of these adjuvants. The vaccine preparation is primarily micrometer-sized clusters of nano-sized particles of the aluminum salt with which the antigen is associated by adsorption and entrapment²¹. The avidity with which the adjuvant associates with the antigen will depend upon multiple factors, including the form of aluminum salt (usually oxyhydroxide or hydroxyphosphate), the physico-chemical properties of the antigen (including its overall charge and molecular weight),

the mode of preparation of the antigen-adjuvant complex (ratio of adjuvant to antigen), and the final solution pH. It appears that proteins bind to aluminum adjuvants in two ways. Probably the most common way is for the proteins to be adsorbed by electrostatic interactions to positively charged aluminum hydroxide. A second method of binding involves 'ligand exchange' between hydroxyl and phosphate groups, like hydroxyl groups of proteins and aluminum phosphates. It has also been demonstrated to occur between aluminum hydroxide and proteins containing phosphate groups²². Once the antigen had been adsorbed by the aluminum salt adjuvant a variable proportion of antigen, often <1% of the total antigen loaded, is not associated directly with the adjuvant²¹.

Aluminum – containing adjuvants induce a strong innate immune response at the sight of injection that consists of an increase of natural killer (NK) cells, neutrophils, eosinophils, CD11b+ monocytes, and dendritic cells (DCs)²³. The infiltration of phagocytes will phagocytize the unlimited diet of particulate aluminum adjuvants at the injection site and will 'eat' until they die, thereby releasing various damage-associated molecular patterns (DAMPs). The next line of phagocytosing cells will thus encounter an environment rich in both adjuvant and DAMPs, increasing the possibility of activation of the Nalp3 inflammasome, and the production of IL-1 β , and thus, inducing inflammation and increasing recruitment, activation, and maturation of immune competent cells²¹. The inflammation process mediates a link between the innate and adaptive immune response by providing an environment essential for the induction of an adaptive immune response²¹.

2.2: Other Types of Adjuvants

Over the decades, a better understanding of the immune response and how adjuvants interact with the immune system has led to new classes of adjuvants. One alternative adjuvant is an emulsions/surfactants mixture. Emulsions are two liquids not capable of mixing that are stabilized with an emulsifier or surfactant. Three well-known examples are complete Freund's adjuvant (CFA), incomplete Freund's adjuvant (IFA) and MF59. MF59 consists of an oil (squalene)-in-water nano-emulsion composed of < 250nm droplets. MF59 is used in Europe as an adjuvant for influenza vaccines and has even been tested in some herpes simplex virus, HBV and HIV antigens²⁰. MF59 is safe for human use and has shown with several antigens to generate higher antibody titers with more IgG1:IgG2a responses than compared to Alum. Also seen were stronger helper T-cell responses when used in vaccination²⁰. It is thought that MF59 acts through a depot and direct stimulation of cytokines and chemokine production by monocytes, macrophages and granulocytes. Like Alum, MF59 does not increase CD4+ Th1 immune responses, but increases haemagglutination inhibiting antibodies and CD8+ T-cell responses, which makes it a good candidate for use in pandemic influenza vaccines²⁰.

Toll-like receptor (TLR) agonists are another class of adjuvants; monophosphoryl lipid A (MPL) is a TLR4 agonists used in licensed vaccines¹⁹. MPL is a non-toxic derivative of the lipopolysaccharide (LPS) of *Salmonella minnesota*, and is a potent stimulator of Th1 responses. LPS consists of two basic structures: a hydrophilic polysaccharide portion and a hydrophobic lipid moiety called lipid A. The lipid A portion can be highly endotoxic but can be that can be reduced by defined structural groups or

varying the number and length of its acyl chains²⁰. The structural changes to the lipid A molecule alter the shape and structural order of the lipid, which influences its aggregation and prevents it from being toxic. In addition, as a TLR4 agonist, structural alterations of lipid A influence its binding affinity as a ligand for TLR4²⁰. MPL is capable of activating T-cell effector responses. TLR agonists employ a directed receptor-mediated mechanism through specific signaling, leading to activation of antigen presenting cells. The combination of antigen presenting cells and antigen presentation leads to adaptive immune responses¹⁹. ASO4 is an aqueous formulation of MPL and Alum, resulting in higher levels of specific antibody and efficacy with fewer injections.

Liposome adjuvants are self-assembling biodegradable and nontoxic phospholipids. Liposomes can encapsulate antigen within the core for delivery and incorporate viral envelope glycoproteins to form virosomes. Liposomes are able to co-deliver both antigen and adjuvant to the same antigen presenting cell, which is crucial for inducing potent immune response. The physiochemical properties such as surface charge, lipid composition and bilayer rigidity highly influence liposome biodistribution and persistence. These parameters can be tuned to elicit a specific type and strength of the immune response. In addition, liposome can protect the antigens from degradation, enhance their uptake by antigen presenting cells, promote release into the cytosol, and even serve as an immunostimulatory function²⁴. Virosomes, a type of liposome, are a relatively new option for vaccine adjuvants. Virosomes are empty reconstituted influenza virus envelopes, and because they contain hemagglutinin, they can bind sialic acid on DCs and macrophages, thereby enhancing antigen availability to, and uptake by, these cells²⁵.

Their mode of action has been described as being through endosomal fusogenic properties that enable them to present antigens in the cytosol in the context of the MHC class I antigen presentation system. Therefore, they can stimulate CD8+ T-cell activity, in addition to stimulating a humoral response and enhanced antigen presentation^{19,25}.

Virus-like particles (VLP) are self-assembling particles composed of one or more viral proteins, resulting in the formation of nanoparticles 20-100 nm in size. VLPs used in vaccines can be broadly divided into two classes: in one class, VLPs that comprise the viral protein subunits that form the viral capsid in nature; and in another class, synthetic VLPs that are derived by the chemical synthesis of pre-designed subunits. VLP are particulate viral entities displaying the conformationally complete viral antigens on their surface but lacking the genetic material necessary for viral replication^{19,20,26}. VLPs can be produced either without modification or by genetically engineering the viral capsid subunit by bioconjugation of the viral capsid subunit with antigenic peptides or other ligands or by site-directed mutagenesis of the intact VLP to create a functional scaffold for multivalent surface presentation of antigens²⁶.

3.0: Nanoparticle vaccine delivery vehicles

The use of nanoparticles as delivery systems and adjuvants has been gaining an increasing amount of interest. Studies show that the use of these particles allows for a more direct delivery of the vaccine to the area of interest, a more specific and stronger immune response to the vaccine, and a time-release capability of the vaccine.

Nanoparticles, because of their size similarity to cellular components, can enter living cells using the cellular endocytosis mechanism. The vaccine antigen is either

encapsulated within or attached onto the surface of the nanoparticle. Conjugation of antigens onto NPs can allow presentation of the immunogen to the immune system in much the same way that it would be presented by the pathogen, thereby provoking a similar response. Moreover, NPs made from some composites enable not only site directed delivery of antigens but also prolong the release of antigens maximizing its exposure to the immune system²⁷.

Vaccine formulations comprising nanoparticles and antigens can be classified by nanoparticle action into those based on delivery system or immune potentiator approaches. As a delivery system, nanoparticles can deliver antigen to the cells of the immune system, i.e. the antigen and nanoparticle are co-ingested by the immune cell, or act as a transient delivery system, i.e. protect the antigen and then release it at the target location²⁸. For nanoparticles to function as a delivery system, association of antigen and nanoparticle is typically necessary. For immune potentiator approaches, nanoparticles activate certain immune pathways that might then enhance antigen processing and improve immunogenicity. For nanoparticle to act as a delivery system antigen attachment is generally achieved through simple physical adsorption or more complex method, such as chemical conjugation or encapsulation. Adsorption of antigen onto a nanoparticle is generally based simply on charge or hydrophobic interaction. Therefore, the interaction between nanoparticle and antigen is relatively weak, which may lead to rapid disassociation of antigen and nanoparticle *in vivo*²⁸. Encapsulation and chemical conjugation provide for stronger interaction between nanoparticle and antigen. In encapsulation, antigens are mixed with nanoparticles precursors during synthesis,

resulting in encapsulation of antigen when the precursors particulate into a nanoparticle. In general, antigen is released only when the nanoparticle has been decomposed *in vivo* or inside the cell. For chemical conjugation, antigen is chemically cross-linked to the surface of a nanoparticle. Antigen is then taken up by the cell together with the nanoparticle and is then released inside the cell²⁸.

For nanoparticles to act as an immune potentiator, attachment or interaction between the nanoparticle and antigen is not necessary, and may be undesirable in case where modification of antigenic structure occurs at the nanoparticle interface. Formulation of immune potentiator nanoparticles with target antigen could be through simple mixing of nanoparticle and adjuvant, shortly prior to injection, with minimal association between nanoparticle and antigen needed²⁸.

Generally, nanoparticles having a comparable size to pathogens can be easily recognized and are consequently taken up efficiently by antigen presenting cells for induction of immune response. DCs preferentially uptake virus-sized particles that are about 20-200 nm while macrophages preferentially uptake larger particles about 0.5-5 μm ²⁸. In addition to particle size, surface charge also plays a role in the activation of immune response. Cationic nanoparticles have been shown to induce higher APC uptake due to electrostatic interactions with anion cell membranes.

3.1: Hydrogel Nanotrap Nanoparticle

Hydrogels are three-dimensional cross-linked polymeric networks that take up large amounts of water¹⁴. They are usually formed through polymerization in the presence of a cross-linking agent¹⁴. Poly(N-isopropylacrylamide) (pNIPAm) based

nanoparticles have been extensively studied and are appealing for drug delivery due to their stability, uniformity, and versatility with regards to the ease of making physical-chemical changes in the particles¹⁴.

The nanoparticles (NPs) have high binding capacity towards the antigen and can slowly release the captured antigen in a controlled manner. NPs are prime candidates as a delivery system due to their ability to capture great amounts of antigen and to slowly release the trapped antigen with kinetics controlled by a quantifiable dissociation rate²⁹. The interaction of the antigen with the high affinity baits also protects the loaded antigen from degradation, making these nanoparticles ideal vaccine adjuvants²⁹⁻³³. These NPs were produced via precipitation polymerization with pNIPAm and methylenebisacrylamide (BIS) and the functionalization of different chemical dye bait using either allylamine or acrylic acid incorporated with the NPs²⁹. The unique property of these hydrogel NPs is the covalent incorporation of high affinity chemical baits ($K_D < 10^{-13} \text{M}$)^{1,3,32}. The chemical baits within the particles core possess extremely high affinity for select types of proteins and peptides. The open-meshwork core nanoparticle and the combination of the chemical baits allow the hydrogel nanoparticles to exclude unwanted particles and capture only the desired ones. The baits also protect the sequestered protein from any degradation, such as degradation from proteases. Even though it is still unclear, the proposed mechanism to explain the high-affinity binding of the chemical baits to proteins is based on hydrophobic and electrostatic forces³³. The specificity of the bait-protein interaction depends mainly on hydrophobic interactions and the electrostatic forces stabilizing the interaction³³. The bait binding site on the surface of the target

protein is thought to be a nonpolar pocket surrounded by hydrophilic amino acid residues³³. The baits are then able to insert aromatic rings into nonpolar hydrophobic pockets of the protein surface³³.

NPs are able to deliver their cargo to dendritic cells (DCs) in a targeted and prolonged manner. Due to their small size, DCs are more readily able to uptake these NPs, inducing an immune response³⁰. Hydrogel nanoparticles can be carried to the lymph nodes, where they are brought to areas of the lymph node that favor interaction of nanoparticle with macrophage and dendritic cell²⁹.

CHAPTER TWO: PRODUCTION AND VALIDATION OF HYDROGEL NANOTRAP NANOPARTICLES TO CAPTURE CHIKUNGUNYA

Hydrogel nanoparticles have been vastly studied as adjuvants and vaccine delivery systems and have shown to be excellent candidates. Hydrogel nanoparticles are the ideal for vaccine manufacturing because they are cheap to manufacture, they are nontoxic, and are able to enhance the immune response to the vaccine. With hydrogel nanotrap nanoparticles specifically, the chemical bait that is covalently bond to the particles core is able to capture the vaccine and deliver it to areas where macrophages and dendritic cells reside.

1.0: Introduction

For adjuvants to be successful they must create a more enhanced immune response than the vaccine alone without being toxic to the body. Most adjuvants in someway adhere to the vaccine or the adjuvant encapsulates the vaccine, making it easier to deliver the vaccine to specific areas or immune cells. Based on past studies, hydrogel nanoparticles have been shown to the capture whole virus and have the ability to be loaded with cargo that can be delivered to the lymph nodes and be presented to immune cells³⁴. Hydrogel nanoparticle core is formed from a precipitation polymerization with pNIPAm and BIS. Within the core is a chemical bait is covalent bound using either

allylamine or acrylic acid. This unique bait has a high affinity for select types of proteins and peptides, making it ideal as an adjuvant for a whole virus vaccine³⁴.

These nanoparticles were screened for their capability to capture whole CHIKV. Since these particles will be used in mouse trials, finding a way to ensure sterility is crucial. The particles are too large to be filtered through a 0.22 μm filter so they were autoclaved. Both pre - autoclaved and post - autoclaved particle size was characterized using a NanoSight. The autoclaved nanoparticles were further characterized by plaque assay to demonstrate that the nanoparticles maintained their ability to capture virus. A time - release study was also conducted to see how well the nanoparticle held on to the captured virus.

2.0 Methods

2.1: Production of nanoparticles

Nanoparticles incorporating dyes remazol brilliant blue R (RBB) and disperse yellow 3 (DY3) were produced. To produce NPs covalently functionalized with RBB, 4.5 grams of *N*-Isopropylacrylamide and 0.07g (for 1% BIS) or 0.14g (for 2% BIS) of *N,N'*-methylene bisacrylamide were dissolved in 125mLs of water, filtered using a 0.45 μm nitrocellulose membrane disk filter, and transferred in a three-neck round bottom flask. The solution was purged for 30 minutes under nitrogen, at medium stirring at room temperature. 338g of allylamine was added, the solution was held for 15 minutes under nitrogen atmosphere at room temperature, and then heated to 70°C and held for 30 minutes. 0.05g of potassium persulfate was dissolved in 3 mLs of water and added to the

solution to initiate the polymerization. The reaction was maintained at 70°C under nitrogen for 6 hours. Particles were washed five times by centrifugation (19,000 rcf, 1 hour, 25°C) to eliminate the unreacted monomer and then resuspended in 300 mL of water. To stain the particles, 1.06g of Na₂CO₃ was dissolved in 80 µL of water. In that solution, 3 g of RBB was also dissolved and then filtered under vacuum with a 0.22µm filter unit. Once the dye was filtered, 100 µL of the particle suspension was mixed with the filtered dye; the suspension was held at room temperature at medium stirring for 48 hours.

For the production of the DY3 nanoparticles, 4.75g of *N*-Isopropylacrylamide and 0.4 g of N,N'-methylene bisacrylamide were dissolved in 500 mL of water, filtered using a using a 0.45µm nitrocellulose membrane disk filter, and transferred in a three-neck round bottom flask. The solution was purged for 30 minutes under nitrogen, at medium stirring at room temperature. 500 of Acrylic Acid was added, the solution was held for 15 minutes under nitrogen atmosphere at room temperature, heated to 70°C and held for 30 minutes. 0.276g of potassium persulfate was dissolved in 5 mLs of water and added to the solution to initiate the polymerization. The reaction was maintained at 70°C under nitrogen for 6 hours. Particles were washed five times by centrifugation (19,000 rcf, 1 hour, 25°C) to eliminate the unreacted monomer and then re-suspended in 600 mL of water. Prior to staining, a preliminary activation of the carboxylic group present in the nanoparticles was performed by centrifuging (16.1 rcf, 25C, 15mins) 20 mLs of the poly(NIPAm-co-AA) particles suspension, discarding the supernatant and re-suspending the pellet in 20 mL of 0.2 M NaH₂PO₄ pH 5. The particle suspension was transferred to a

three-neck round flask, and 2 mL of 1% SDS, 1.648 g of N-(3 dimethylaminopropyl)-N'-ethyl carbodiimide hydrochloride, and 1.224g of solid N-hydroxy succinimide were added to the solution. The reaction was held at room temperature for 15 minutes. The suspension was then centrifuged (19,000 rcf, 1 hour, 25°C), the supernatant was discarded, and the particle pellet was re-suspended in 40 mL of 0.2 M Na₂HPO₄ pH >8. After this activation step, a molar ratio of dye/ Acrylic Acid 10:1 was dissolved in 360 mL of 0.2 M NaHPO₄ buffer pH 8 >8, which was filtered by 0.22 µm CA filter and added to the activated particles. The reaction was held at room temperature at medium stirring overnight. To eliminate the unreacted dye, poly (NIPAm/dye) particles were washed five times with water by centrifugation (19,00 rcf, 1 hour, 25°C). Supernatants were discarded, and particles were resuspended in 20 mL of water.

2.2: Validate nanoparticles with purified inactivated CHIKV through Plaque Assay

The vaccine, whole CHIK PIV vaccine strain 181-25, was manufactured at the WRIAR Pilot Bioproduction Facility by Clinical Research Management (Silver Spring, MD, USA) according to good manufacturing practices. 10 mL of each nanoparticle was aliquoted out and autoclaved. Once the nanoparticles were cooled, 375 µL of each of the nanoparticles was incubated with 500 µL of purified attenuated CHIKV virus for 30 minutes at room temperature. After the incubation period, the samples will be centrifuged for 5 minutes at 10,000 rcf, at 4° C. The supernatant was separated from the pellet and the pellet resuspended with 500 µL of 1x PBS.

For the plaque assay, 12-well plates were seeded with Vero-WHO cells at a cell density of 5.0×10^5 cells/mL. 1.5 mL of the cell suspension was added to each well. The plates were incubated in a $5 \pm 1\%$ CO₂ incubator at $35 \pm 2^\circ\text{C}$ and greater than 95% relative humidity until the cells reached confluence (about 48 hours). After the two-day incubation period the CHIKV standard positive control, CHIK vaccine positive control, nanoparticle control and samples were prepared in a diluent consisting of EMEM, 1% heat-inactivated FBS, 1% streptomycin, and 0.5% neomycin. CHIKV standard control was serial diluted ten-fold up to 10^6 . The vaccine positive control was serial diluted up to 10^3 . Each nanoparticle-vaccine pellet was serial diluted up to 10^4 and the supernatant was serial diluted up to 10^2 . Plates were decanted and 100 μL of the inoculum was added to each well. Dilutions 10^4 , 10^5 , 10^6 of the CHIKV standard positive control, 10^2 and 10^3 of the vaccine control, undiluted for the nanoparticle control, 10^2 , 10^3 , 10^4 of the nanoparticle-vaccine pellets, and 10^2 and 10^3 of the nanoparticle-vaccine supernatants were plated. The plates were then incubated for 1 hour in a humidified, $5 \pm 1\%$ CO₂ incubator at $35 \pm 2^\circ\text{C}$ to allow virus adsorption. After the hour incubation 1.5 mL/well of an overlay solution was added. Plates were incubated for 2 days in a humidified, $35 \pm 2^\circ\text{C}$, 5% CO₂ incubators. After the 2 day incubation period, the plates were decanted and carefully rinsed with RODI water then decanted again. The cells were then fix-stained by filling each well with 1.0 mL of Naphthol blue black staining solution. The plates were incubated for 10-15 minutes at $18-25^\circ\text{C}$. Plates were then decanted and washed with RODI water. Once plates were dry the plaques were counted.

2.3: Size characterization of nanoparticle

Autoclaved DY3 nanoparticles were diluted 4.0×10^6 fold; pre-autoclaved DY3 nanoparticles were diluted 400 fold; autoclaved RBB 1% BIS nanoparticles were diluted 100 fold; pre-autoclaved RBB 1% BIS NPs were diluted 100 fold; autoclaved RBB 2% BIS NPs were diluted 1000 fold; pre-autoclaved RBB 2% BIS NPs were diluted 1000 fold. Each sample was loaded into the sample chamber (Luer fitting) using a syringe without a needle. Once the sample was loaded, the LM10 unit was placed onto the microscope stage and a video to analyze particle size was taken using a Nanosight (Malvern).


2.4: Time-release study of CHIKV with selected nanoparticles

The time-release study was only conducted on the nanoparticle that was to be used in the mouse trial. 7.5 mL of RBB 2% BIS NPs was incubated at room temperature for 30 minutes with 10 mL of CHIK PIV vaccine. After incubation, the sample was centrifuged for 5 minutes at 10,000 rcf at 4° C. The supernatant was removed and the pellet re-suspended with 17.5 mL of 1xPBS to initiate the dissociation of the CHIK PIV. On Day 0, 24 hours, Day 7, Day 14, Day 21, and Day 28, aliquots were taken from the nanoparticle/CHIK PIV suspension and centrifuged for 5 minutes at 10,000 rcf. The supernatant was removed and saved for testing by ELISA.

Sensitized 96-well microplates were coated with 100 µL/well/sample. 1xPBS was used as a blank, the nanoparticle/CHIK PIV supernatant sample was 2 fold serial diluted with PBS and nanoparticle supernatant was used as a negative control and serial diluted

with PBS. The nanoparticle/CHIK PIV samples were tested in triplicate. **Figure 1** shows the plate layout.

A.

	1	2	3	4	5	6	7	8	9	10	11	12
A	BLANK	POSITIVE CONTROL (CHIK PIV)										BLANK
B												
C		SAMPLE										
D												
E		SAMPLE										
F												
G		SAMPLE										
H												
2x serial dilution 												

B.

	1	2	3	4	5	6	7	8	9	10	11	12
A	BLANK	Supernatant of RBB NP										BLANK
B												
C		BLANK										
D												
E		BLANK										

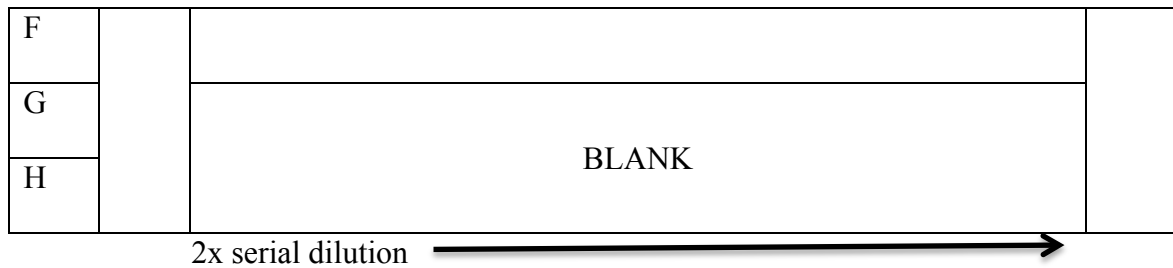


Figure 1. 96-well ELISA plate layout. A) Positive control and sample was serial diluted 2 fold. The samples were tested in triplicate. Column 1 and 12 were used as blanks. B) This plate was used as a negative control for the NPS. The supernatant of the RBB nanoparticles alone was plated and serial diluted. Column 1 and 12 were used as blanks.

The coated plates were incubated at 2-8°C for 1-3 days. After the established coating period the plates were taken out of the incubator and washed 2 times with 100 µL of wash buffer (0.05% Tween in 1xPBS). The plates were then coated with 300 µL of an antibody blocking diluent and placed in a 20-25 °C incubator for 30 minutes. The plates were then washed 2 times with 100 µL of wash buffer. 100 µL of the primary antibody was added to all wells and the plate was incubated for 2 hours at 30-35 °C. The primary antibody used was a mouse-anti-CHIKV sera polyclonal detecting antibody, diluted 800 fold with antibody blocking diluent.

After the two-hour incubation period the plates were washed 5 times with 100 µL of wash buffer and then coated with 100 µL/well of the secondary antibody and then incubated for 1 hour at 30-35 °C. Goat-anti-mouse-HRP was used as the secondary antibody, diluted 6,000 fold with antibody locking diluent. The plates were then washed 5

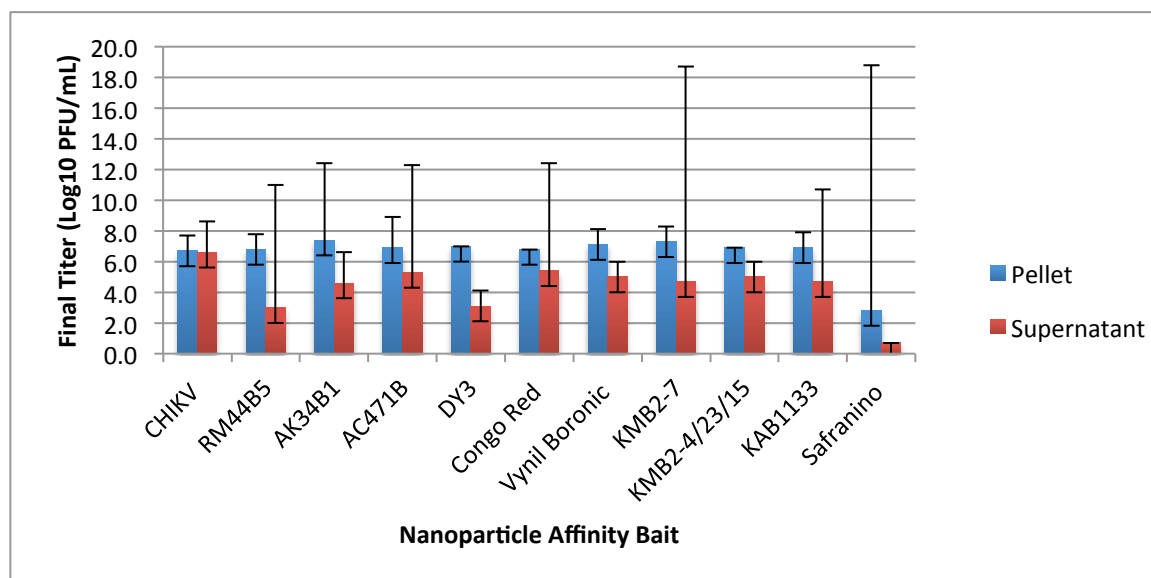
times with 100 μ L of wash buffer and coated with 50 μ L/well of Sure Blue TMB HRP substrate. The plates were incubated at room temperature (20-25°C) in the dark for 5-15 minutes. After the incubation period 50 μ L/well of a stopping solution (1:25 phosphoric acid) was added. The plates were then read at 450nm.

3.0 Results

3.1: Nanoparticles captured CHIK virus

An initial screening was conducted to see whether or not the hydrogel nanoparticles had the capability to capture a whole chikungunya virus vaccine, **Figure 2**. Ten hydrogel nanoparticles with different chemical baits were individually screen with purified attenuated chikungunya virus strain 181-25 in order to identify the top affinity bait nanoparticles that can capture the most live attenuated virus. Based on the percent capture, two nanoparticles were chosen as top candidates for a novel adjuvant for a purified inactivated whole chikungunya virus vaccine. To see if more whole virus could be captured, nanoparticles were synthesized with two different BIS percentages, 2% BIS and 1% BIS. The 1% BIS nanoparticle has slightly larger pore size in the nanoparticle core compared to the 2% BIS due to less cross-linking between the BIS and pNIPAm.

A.



B.

NPs	% Capture
RM44B5	69%
AK34B1	62%
AC471B	19%
DY3	69%
Congo Red	56%
Vynil Boronic	59%
KMB2-7	61%
KMB2-4/23/15	58%
KAB1133	59%
Safranino	80%

Nanoparticle Affinity Bait	Fold Change (Log10)
CHIKV	0.1
RM44B5	3.8
AK34B1	2.8
AC471B	1.6
DY3	3.9
Congo Red	1.4
Vinyl Boronic	2.1
KMB2-7	2.6
KMB2-4/23/15	1.9
KAB1133	2.2
Safranino	2.1

29

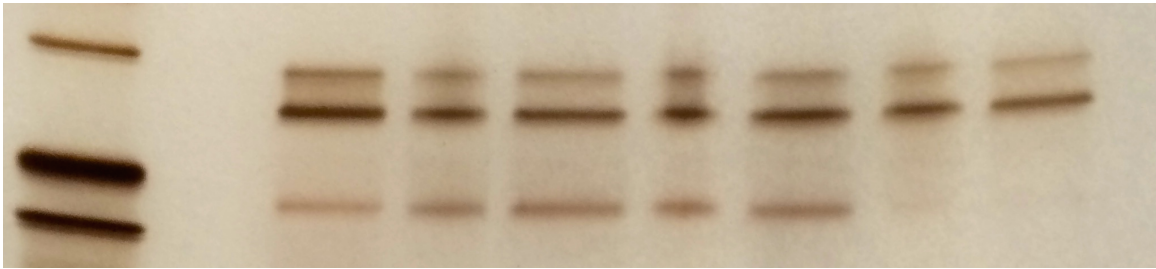


Figure 2. Nanoparticle screening with CHIKV Results. A) The virus titer in Log_{10} PFU/mL for each nanoparticle pellet and supernatant that was incubated with CHIKV. The graph shows the amount of virus captured by the nanoparticle, represented in the pellet (blue column), and the amount of virus that was left in the supernatant (red column). B) The percent capture of whole virus by the nanoparticles. DY3 NP and RM44B5 had the highest percent capture; DY3 had 69% capture of the virus and RM44B5 also had 69% capture. Nanoparticle Safranino shows a falsely percent capture. The Safranino particle interacts with the virus in a way that alters the virus itself. C) The fold difference in Log_{10} between the virus captured in the nanoparticle pellet and the supernatant. Nanoparticle Safranino also shows a falsely high fold difference. D) Silver stain SDS-PAGE demonstrates the ability of several dye-functionalized hydrogel nanoparticles to captured CHIK virus. SUP = supernatant.

3.2: Size characterization of nanoparticle before and after autoclaving.

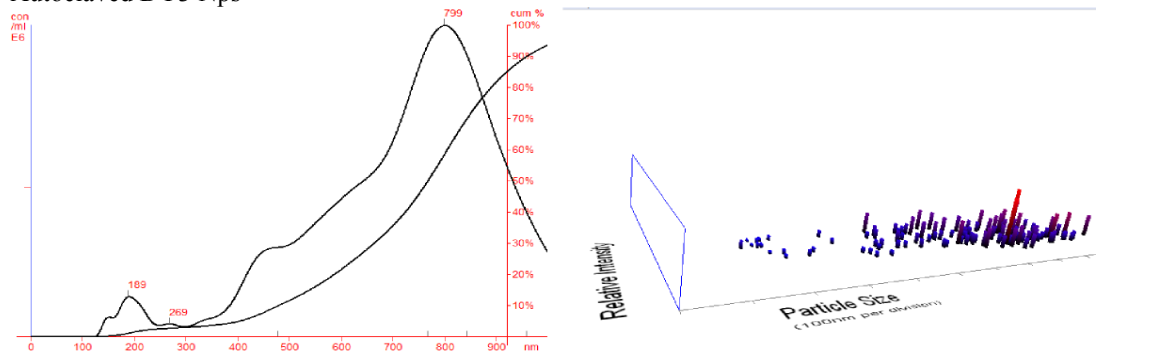
Figure 3 shows concentration particle sizes and relative intensity 3D plot for each particle. For the autoclaved DY3, the mode was 799 nm and the mean was 742 nm. The pre-autoclaved DY3 had a mode of 866 nm and mean of 822 nm. There was a small

subset of 189 nm particles in the autoclaved DY3, which could be the color dye that was incorporated initially into the particles core and could account for the loss in color.

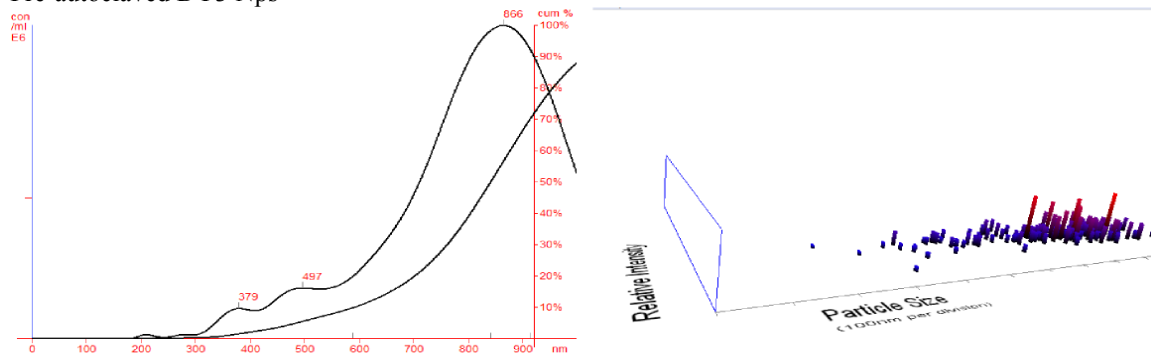
Interestingly, the autoclaved DY3 particles were 1×10^4 more concentrated compared to the non-autoclaved particles.

The mean for the autoclaved RBB 1% BIS NPs was 331 nm and the mode was 294 nm. For the non-autoclaved RBB 1% BIS NPs, the mean was 302 nm and the mode was 306 nm. The autoclaved RBB 2% BIS NPs had a mean of 417 nm and a mode of 439 nm. The non-autoclaved RBB 2% BIS NPs had a mean of 390 nm and a mode of 397 nm.

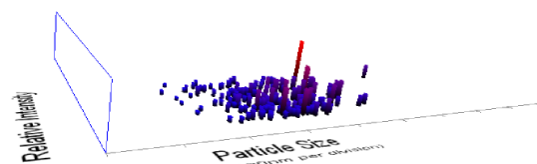
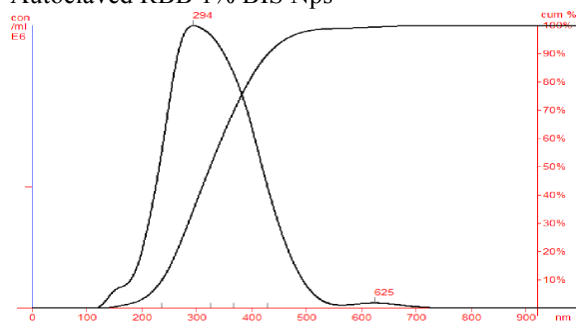
Autoclaved DY3 Nps



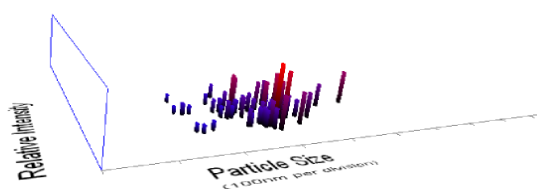
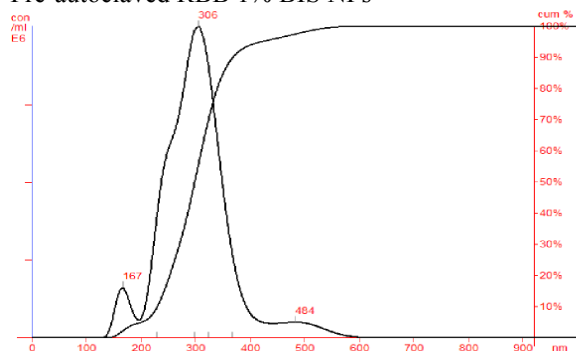
Pre-autoclaved DY3 Nps



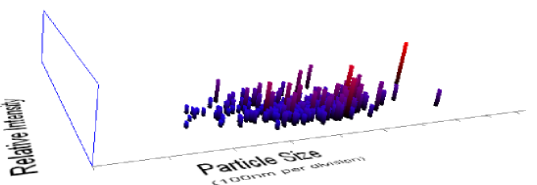
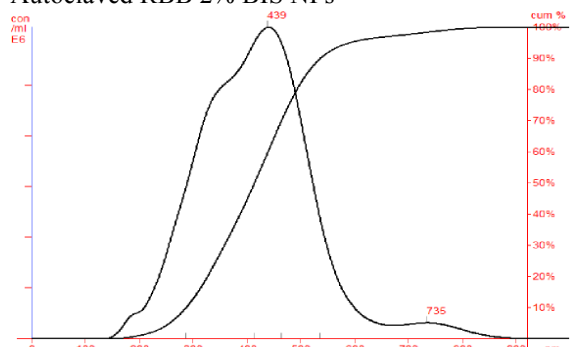
Autoclaved RBB 1% BIS Nps



Pre-autoclaved RBB 1% BIS NPs



Autoclaved RBB 2% BIS NPs



Pre-autoclaved RBB 1% BIS NPs

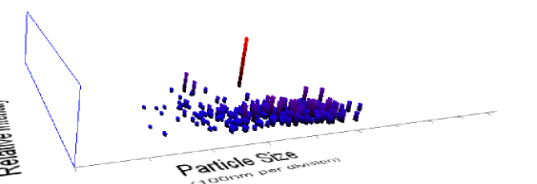
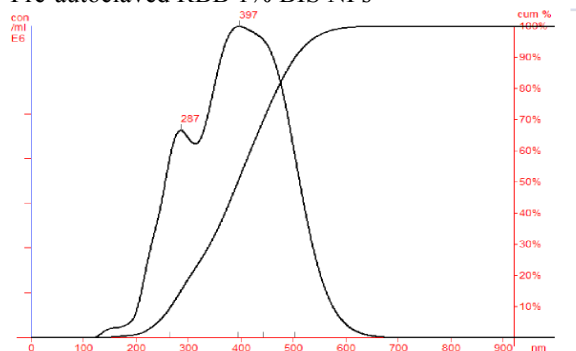


Figure 3. NanoSight Characterization of non-autoclaved and autoclaved NP. Particle Size / Concentration Particle Size / Relative Intensity 3D plot of DY3 particle (**top two graphs**), RBB 1% BIS (**middle two graphs**) and RBB 2% BIS (**bottom two graphs**), before autoclaving and after autoclaving.

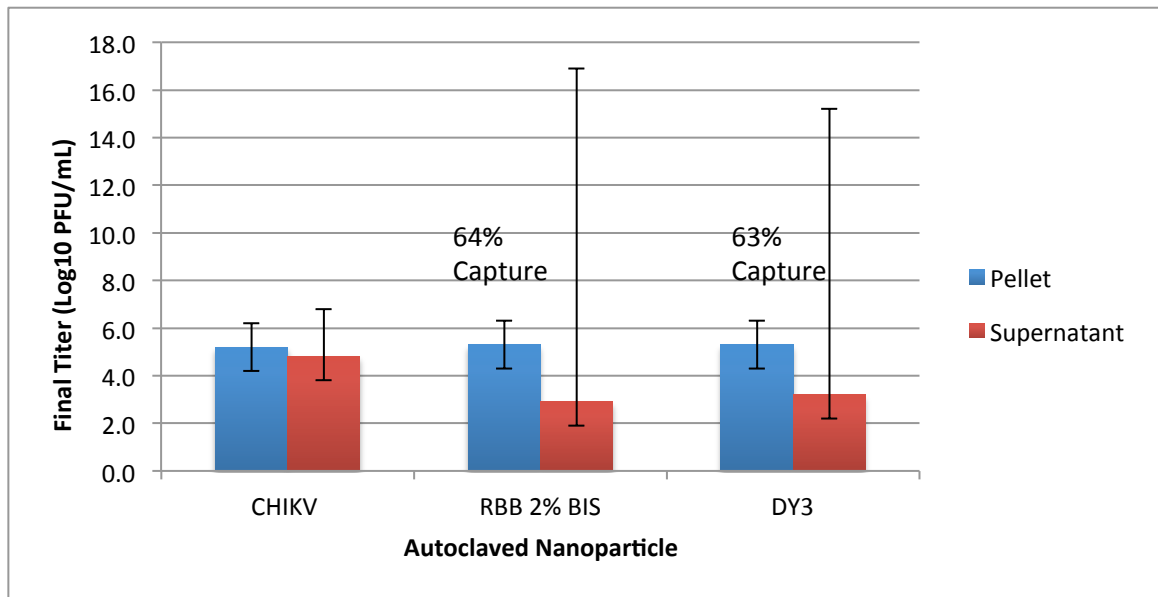
3.3: Autoclaved nanoparticles are able to capture virus.

The NPs we synthesized are based on poly(N-isopropylacrylamide) (pNIPAm) and methylenebisacrylamide as a cross-linker co-polymerized with allylamine or acrylic acid (AAc,) for incorporation of different chemical baits. a

All three particles were able to capture virus once autoclaved, **Figure 4**. The final titer in the pellet for autoclaved RBB 2% BIS was 5.2 Log₁₀ PFU/mL and the supernatant titer was 2.9 Log₁₀ PFU/mL, with a 2.4 fold difference between captured virus in pellet and remaining virus in supernatant. The percent capture for the RBB 2% BIS was 64%. For the autoclaved 1% BIS RBB NP the pellet titer came to 5.1 Log₁₀ PFU/mL and the supernatant titer was 3.1 Log₁₀ PFU/mL, fold difference of 2. The DY3 autoclaved particle pellet had a titer of 5.3 Log₁₀ PFU/mL and the supernatant had a titer of 3.2 log₁₀ PFU/mL, fold difference of 2.1. The DY3 percent capture came to 63%. There was a decrease in the amount of virus captured with the autoclaved particles compared to the pre-autoclaved particles. **Figure 4** shows the fold difference between the pre-autoclaved NPs and the post-autoclaved. The drop in fold change could be due to

physico chemical modifications of the polymer meshwork or of the chemical baits in the nanoparticles.

A.



B.

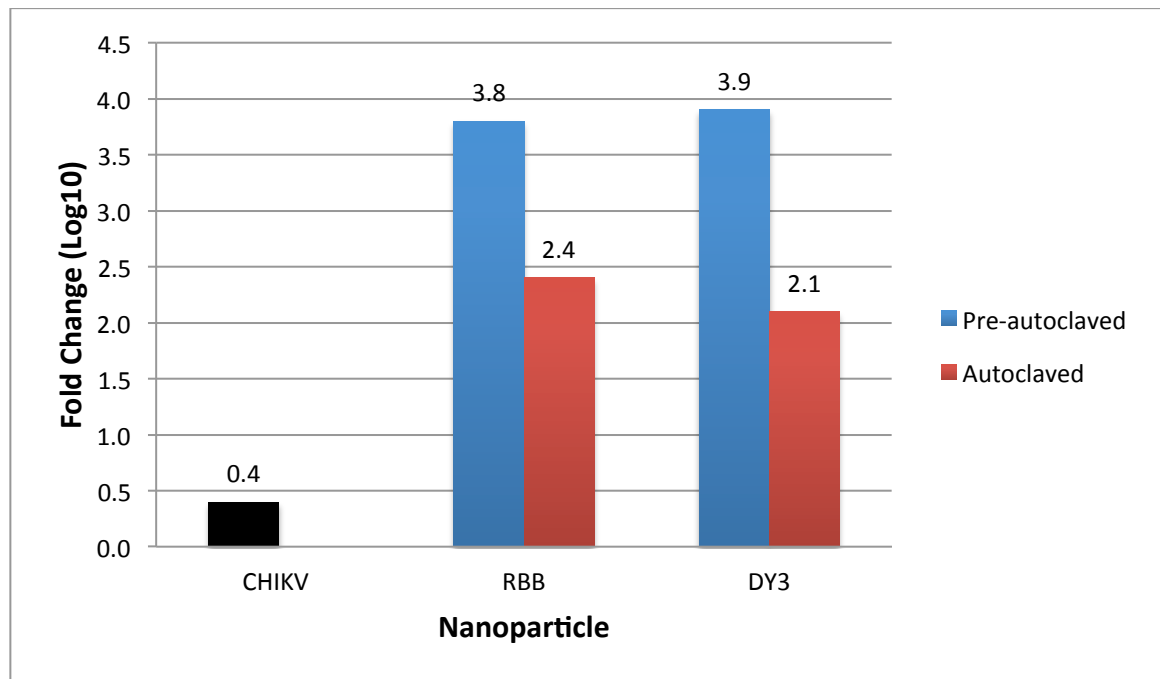


Figure 4. Plaque assay results of the autoclaved nanoparticles. A) Final virus titer in the pellet and supernatant for the autoclaved nanoparticles. The blue column represents the virus captured in the pellet and the red column represents the unbound virus. B) Fold change between virus captured in the pellet the in NP supernatant compared to the fold change in virus titer in the pre-autoclaved particles. The fold difference between the pre-autoclaved RBB and DY3 particles did not vary significantly and same with the fold difference between the autoclave RBB and DY3 particles. There was a difference in virus captured between the pre and post-autoclaved NPs.

3.4: The selected nanoparticle is adsorbed to vaccine and is not released

To test the CHIK PIV release rate the NPs were loaded with CHIK PIV at room temperature for 30 minutes and then pelleted to remove supernatant (Sup). The NPs were then re-suspended in an equal volume of PBS to the initial volume to initiate the CHIK PIV dissociation, and the suspension was incubated at 4°C. The NPs from the aliquots of this suspension corresponding to a certain fraction of the total volume were pelleted and the amount of released CHIK PIV in the Sup was determined by ELISA with a mouse-anti-CHIKV sera polyclonal detecting antibody. An equal fraction of the total CHIK PIV amount used for loading served as a control representing 100% release of the vaccine and an equal fraction of the NP sup was used as negative control representing 100% captured of the vaccine. At every time-point the sup showed no release of the vaccine. The NP sup was also tested to show that it did not cause any false signal. **Figure 5** shows that the sup of the NP and the sup from each time-point had an extremely low signal, equivalent to the blank. Time =0 hr through Time=Day 28 all were <2 EU. **Figure 5** shows that the NPs held onto their cargo for the entire length on the study.

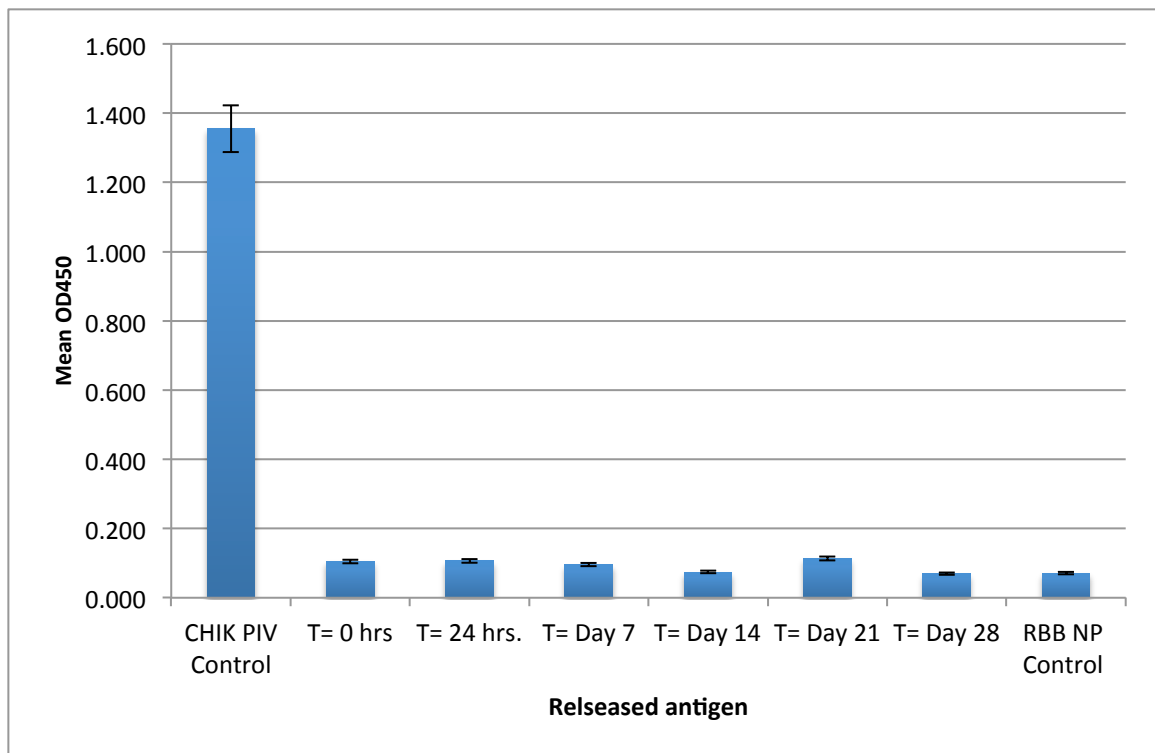


Figure 5. Time-release study. Release of adsorbed CHIK PIV to RBB 2% BIS. CHIK PIV (14 $\mu\text{g/mL}$) was mixed with indicated NP and incubated at room temperature for 30 minutes. After incubation the NPs were pelleted for 5 min at 10,000 rcf and room temperature, re-suspended with PBS, and incubated at 4 $^{\circ}\text{C}$. Portions of the suspension were withdrawn at indicated times, the NPs were pelleted for 5 min at 10,000 rcf, and supernatants removed. The amount of CHIK PIV released in the supernatants were determined by ELISA.

4.0 Discussion

The NPs capable of capturing whole virus vaccine hold promise for a novel adjuvant for virus vaccines³⁴. An ideal adjuvant is required to be non-toxic, stable, show no other potential side effects, and be easy to manufacture. The pNIPAm NPs represent an attractive platform offering a possibility to generate non-toxic, sufficiently stable, controlled-porosity hydrogel materials amenable to different chemical modifications²⁹. The incorporation of more than 20 different dye baits allowed the NPs to modify its affinity towards the substances of interest for a variety of applications²⁹. The possibility to capture whole virus vaccine the dye-coupled NPs was explored with the aim of creating nanomaterial that would capture and deliver their cargo to a desired area. Similar to the commonly used aluminum hydroxide adjuvant, the bait affinity NPs allow a possibility of whole virus vaccine to be loaded in mild physiological conditions. In addition, the hydrogel NP matrix protects the loaded whole virus vaccine from proteolytic damage²⁹. The NPs also are able to maintain the captured cargo for an extended period of time *in vitro*, similar to aluminum salt adjuvants. While the exact nature of the dye interactions with target antigens is often unclear, it is thought that the aromatic rings interact with the virus' outer surface.

Different dye-coupled NPs were screened to determine which dye bait had the highest affinity for capturing CHI PIV. RBB and DY3 showed to be the best candidates for capturing whole virus vaccine. RBB was engineered with 2% BIS and 1% BIS. The 1% BIS RBB particle had less crosslinking, therefore large pore size in the core. The idea was the larger pore size in the core would allow more virus to be captured. Based off the

fold change between captured virus in the pelleted nanoparticles and virus remaining in the supernatant for RBB 1% BIS (2 Logs) and for RBB 2% BIS (2.4 Logs), the difference in crosslinking with the BIS did not have any major effect on the amount of captured virus. All the particles were autoclaved for sterilization and their size was characterized by Nanosight. The size between the non-autoclaved NP and the autoclaved NP did not change substantially. The NPs were also visually inspected after they had been autoclaved. The RBB NPs did not seem to have any visual signs of degradation. DY3 NP did have a loss of its coloring after autoclaving. The autoclaved NPs ability to capture whole virus was assessed by plaque assay. **Figure 4** showed a decrease in the amount of virus captured by the autoclaved NPs. The autoclaving could have 1) disrupted the covalent bonds between the dye and the particle core, causing less available dye to bind with the virus or 2) changed stiffness and viscosity of the nanoparticles, creating higher diffusion barriers for the antigen access to the particles.

The time-release study was to determine the release-rate of the selected NP. Commonly used aluminum salt adjuvants adsorb to the vaccine. The prolonged association of vaccine with adjuvant attracts more immune cells to the sight of injection but also acts as a delivery system to bring the vaccine to the desired areas, creating a stronger immune response. Ideally, the NP novel adjuvant would stay associated with the whole virus vaccine till the booster shot in the mice trial. The length of the time-release study was the same length of the mouse trial. The vaccine/NP suspension was tested at T= 0 hr., 24 hrs., Day 7, Day 14, Day 21, and Day 28 and showed no sign the NPs were releasing the vaccine. Surprisingly the time-release study showed was that the RBB 2%

BIS NP maintains its loaded cargo for a prolonged period of time *in vitro*. When the time releases study was initiated and the nanoparticles and captured virus was pelleted and resuspended to initiate the NP-virus dissociation. The volume used to resuspend the pellet was the same as the initial volume of NP and vaccine. This could be a reason for the lack of release of virus vaccine. The pellet should have been resuspended in a much larger volume to push the kinetics of capture and release in the direction of release. Another reason for the lack of release could be the for cell receptor contact with the virus. In the *in vitro* time-release study the nanoparticle never released the antigen. In the plaque assay screening the results showed that the virus entered the cell, was able to replicate and form plaques. It is still unclear if the nanoparticle releases the virus once the virus enters the cell. If the nanoparticle does release the virus once it enters the cell then the time-release data does not accurately represent the release rate of the particle, indicating the need for cell receptor contact with the virus and NP to release the virus.

Overall, the results establish that dye bait-coupled nanoparticles are able to capture a whole virus vaccine and maintain their loaded cargo for an extended period of time *in vitro*. The particles were successfully sterilized for vaccine use and their structure did not appeared to have altered substantially. The next step is to optimize the nanoparticle with the antigen by determining the best antigen-to-NP ratio in order to maximize the percent capture of virus and to determine the optimal time needed for the NPs to adsorb to the antigen. The rate-of-release also needs to be optimized to ensure the best immune response is elicited and the need for cell receptor contact for viral release needs to be determined. So looking at different dye baits that release the antigen at

different rates, looking at immune responses to determine the best way for delivering the vaccine to the desired location and designing an assay that allows cell receptor contact with the NP adjuvanted vaccine.

CHAPTER THREE: INVESTIGATION OF THE IMMUNE RESPONSE OF SELECTED HYDROGEL NANOTRAP NANOPARTICLES AS A NOVEL ADJUVANT FOR A CHIKUNGUNYA VIRUS VACCINE BY MOUSE TRIALS

In order for a vaccine to be a good candidate the vaccine must create a strong immune response. The vaccine must be able to create neutralizing antibodies that will neutralize and help clear the body of the viral antigen if ever exposed to the virus. The vaccine should also create the proper immune response, along with memory of the virus antigen. Memory and neutralization of the viral antigen is a major key when creating a successful vaccine.

1.0 Introduction

Generating vaccine-mediated protection is a complex challenge. A vaccine's early protective efficacy is primarily conferred by the induction of antigen-specific antibodies. However, there is more to antibody-mediated protection than the peak of vaccine-induced antibody titers. The quality of such antibody responses has been identified as a determining factor of efficacy. In addition, long-term protection requires the persistence of vaccine antibodies and/or the generation of immune memory cells capable of rapid and effective reactivation upon subsequent microbial exposure³⁵. The determinants of immune memory induction, as well as the relative contribution of persisting antibodies

and of immune memory to protection against specific diseases, are thus essential parameters of long-term vaccine efficacy³⁵. Current vaccines mostly mediate protection through the induction of highly specific IgG serum antibodies. These IgG antibodies are able to neutralize the virus, preventing the further replication and spread of the disease in the body. Even though the neutralizing antibodies are a good indicator of a protective vaccine, the importance of B and T cell responses in the efficacy of current vaccines should not be over looked.

The induction of antigen-specific B and T cell responses requires their activation by specific antigen presenting cells (APC), essentially dendritic cells (DC), which must be recruited into the reaction. Immature DCs patrol throughout the body³⁵. When exposed to pathogens, they undergo a brisk maturation, modulate specific surface receptors and migrate towards secondary lymph nodes, where the induction of T and B cell responses occurs. The central role for mature DCs in the induction of vaccine responses reflects their unique capacity to provide both antigen-specific and costimulation signals to T cells, ‘danger signals’ required to activate naïve T cells³⁵. The very first requirement to elicit vaccine responses is to provide sufficient danger signals through vaccine antigens and/or adjuvants and to trigger an inflammatory reaction that is mediated by cells of the innate immune system³⁵. Following their activation, DCs migrate towards the local draining lymph nodes³⁵.

B cells are activated in the lymph nodes that have been reached by vaccine antigens, upon diffusion and/or in association to migrating DCs. Protein antigens activate both B and T cells, which results in the induction of a highly efficient B cell differentiation

pathway through specific structures (germinal centers, GCs) in which antigen-specific B cells proliferate and differentiate into antibody-secreting plasma cells or memory B cells³⁵. Antigen-specific plasma cells elicited in spleen/nodes after immunization only have a short life span, such that vaccine antibodies rapidly decline during the first few weeks and months after immunization. A fraction of plasma cells that differentiated into germinal centers however acquire the capacity to migrate towards long-term survival niches mostly located within the bone marrow (BM), from where they may produce vaccine antibodies during extended periods. Memory B cells are generated during primary responses to T-dependent vaccines³⁵. The antigen-driven activation of memory B cells results in their rapid proliferation and differentiation into plasma cells that produce very large amounts of higher-affinity antibodies. As the affinity of surface Ig from memory B cells is increased, their requirements for reactivation are lower than for naïve B cells: memory B cells may thus be recalled by lower amounts of antigen and without CD4⁺ T cell help. Antigen-specific memory cells generated by primary immunization are much more numerous than naïve B cells initially capable of antigen recognition³⁵. The dose of antigen is an important determinant of memory B cell responses. At priming, higher antigen doses generally favor the induction of plasma cells, whereas lower doses may preferentially drive the induction of immune memory³⁵. Thus, a lower antigen content may be preferred if the rapid induction of protection is not required. Closely spaced primary vaccine doses may also be beneficial for early post-primary antibody responses but not for post-booster antibody responses³⁵. The persistence of memory B cells is of utmost importance for long-term vaccine efficacy.

Following CHIKV infection in humans and nonhuman primates (NHPs), the incubation period is typically 3–7 days (range 1–12 days). IgM antibodies can be detected approximately 2–3 days after onset of symptoms, followed by production of IgG antibodies at approximately 1–2 weeks. Neutralizing antibodies offer protection against CHIKV infection/disease in humans and in animal models and persist for many years after infection in humans. Epitope mapping studies with human sera and monoclonal antibodies have identified linear and conformation-dependent epitopes in the E1/E2 glycoproteins, particularly in the region of the exposed trimer spike, that are targets of strongly neutralizing antibodies³⁶. It has also been suggested that early production of neutralizing IgG3 antibodies in particular may protect against chronic arthralgia in humans³⁶. Little is known about the adaptive response to CHIKV and how it plays a role in clearing the disease. Studies have shown that T cells and B cells play a role in the long-term immunity and clearance of the virus. One study suggested that other factors aside from antibodies and IFN α/β , primarily CD4 T cells, are active in CHIKV viraemia suppression³⁷.

2.0 Methods

2.1: mouse study and neutralization antibody assay

On Day 0, four dosage groups of the non-adjuvanted chikungunya virus purified inactivated vaccine (PIV), four dosage groups of the RBB nanoparticle-adjuvanted CHIKV PIV and a placebo were test articles was diluted with diluent (1 x PBS) and administered to mice (ten mice per dilution) subcutaneously (0.2 mL) in the loose skin of the back by a 22 gauge, ¼ to 1-inch needle and 1 mL syringe. The 1xPBS diluent was also used as a placebo. On Day 14 the animals were boosted in an identical manner with the same test articles. On Day 28 the animals were exsanguinated by intra-cardiac bleeding while under Ketamine/Xylazine anesthesia. Individual blood specimens were processed to sera, frozen and shipped back to the laboratory facility.

Monolayers of Vero WHO cells were seeded at 5.0×10^5 cells/mL in 96-well flat bottom plates 100 µL of cell suspension per well. The plates were incubated for 2 days at 35°C, 95% relative humidity and 5% CO². One day prior to testing, the sera samples were dilute 1:10 with growth medium and heat inactivated at 56°C for 30 minutes. One the day of the neutralization assay, 100 µL of growth medium was added to each 96-well round bottom polypropylene plate except for row H and an extra 100 µL of growth medium was added row A 1-9. 150 µL /well of inactivated serum was added to row H in triplicates. Then 6 3-fold serial dilution were performed by transferring 50 µL/well of the initial dilution up through row B. the extra 50 µL from row B was discarded after mixing. Then 100 µL/well of the diluted virus (a virus does of 50 PFU/well of CHIKV) was

added to every row except row A 1-9. Once all the plates had been mixed they were incubated for 2 hours at 35°C. **Figure 6** shows the layout of the 96-well plates.

	1	2	3	4	5	6	7	8	9	10	11	12	Serum Dilution
A	BLANK									Virus Dose			None
B	Sample 1		Sample 2		Sample 3		Sample 4			1:7290			
C	Sample 1		Sample 2		Sample 3		Sample 4			1:2430			
D	Sample 1		Sample 2		Sample 3		Sample 4			1:810			
E	Sample 1		Sample 2		Sample 3		Sample 4			1:270			
F	Sample 1		Sample 2		Sample 3		Sample 4			1:90			
G	Sample 1		Sample 2		Sample 3		Sample 4			1:30			
H	Sample 1		Sample 2		Sample 3		Sample 4			1:10			

Figure 6. 96-well plate layout for the micro neutralization. Each mouse sera sample was plated in triplicates then serially diluted up. Growth media was used as the blank and CHIK virus was used as a positive control. A virus dose of 50 PFU.well of CHIKV was added to all the rows except the blanks.

After the two-hour incubation period the growth medium was decanted from the flat bottom plates and the 200 µL/well from each of the virus/serum neutralization plates was transferred according to the monolayers of Vero WHO cells plates. The plates were

incubated for 4 days at 35°C, 95% relative humidity and 5% CO². After the four-day incubation period the plates were decanted and washed with RODI water. The water was decanted and 100 µL/well of Naphthol blue black stain was added to each plate and incubated for 30 minutes at 20-25°C. The stain was then decanted, plates washed with water and read at 620 nm. The OD data was used to generate geometric mean titers (GMTs) for each vaccine dilution tested and analyzed by Prism's 4-parameter logistics non-linear regression model to determine a median immunizing dose (ID50%).

2.2: Optimization of Cell-mediated immunity test

After the 28-day mouse study, the mice were sacrificed and their spleens were removed. The spleens were placed in a solution of DMEM, 10% DMSO, 10% FBS, and 1% gentamicin and then placed in Mr. Freezy for a slow freeze. The frozen spleens were shipped back to the lab facility on dry ice. To optimize the cell and antigen concentration, one spleen from the non-adjuvanted group and one spleen from the placebo group were used. To thaw the spleens they were placed in 36.9 °C water bath until the liquid was thawed. The cryovials were then placed at room temperature and disinfected by wiping down each vial with 70% isopropanol alcohol.

Thawed spleens were placed in RPMI-10 cell culture media containing Benonase Nuclease (1:1000). The spleen and cell culture media were then dumped over a 70 µm nylon cell strainer sitting over top a clean 50 mL conical tube. The mouse spleen was then mashed through the cell strainer and rinsed with RPMI-10 cell culture media containing Benonase Nuclease and 1x Phram lyse. The cell mixture then sat for about one minute before it was spun for 8 minutes at 300xg. The supernatant was decanted, cell

pellet resuspended with Phram lyse and incubated at room temperature for 3-5 minutes. RPMI-10 cell culture media containing Benonase Nuclease was then added to the cell suspension and spun for 8 minutes at 300 xg, supernatant decanted and resuspended in RPMI-10 containing Benonase Nuclease, this was done a second time but the cell suspension was resuspended in 5 mL of just RPMI-10. Cells were counted using a CTLS6 Universal-V analyzer. Cell suspension then rested for 1 hour.

The ELISpot plate was treated with 35% ethanol for a maximum of 1 minute. Plate contents was discarded and then washed 5 times with dH₂O. Half the plate was then coated with IFN- γ , which stimulates Th1 cells, coating antibody and the other half of the plate was coated a IL-4, which stimulated Th2 cells, coating antibody at a concentration of 15 μ g/mL and incubated over night at 2-8 °C. After the overnight incubation the plate was decanted and washed five times with PBS to remove unbound coating antibody. RPMI-10 was then added for one hour to block non-specific binding. Resting cells were retrieved and spun for 8 minutes at 300xg and resuspended in RPMI-10. Plate was then decanted and cells were added; 2×10^4 placebo cells/well for the placebo, 3×10^4 non-adjuvanted cells/well for the non-adjuvanted and then 3.5 μ g/mL/well of CHIK PIV antigen was added. Plate was incubated at 37°C over night. The following day the detection antibody was prepared in PBS containing 0.5% FBS, according to Mabtech's kit instruction manual, and passed the entire solution through a 0.2 μ m filter system. The ELISPot plate was removed from the incubator, decanted and washed five times with PBS. The detecting antibody solution was added to the plate and incubated at room temperature for two hours. A 1:1000 dilution of streptavidin-conjugated enzyme in PBS

containing 0.5% FBS was prepared. After incubation the plate was decanted and washed five times with PBS. The streptavidin-conjugates enzyme solution was added and incubated at room temperature for one hour. A TMB substrate was filtered through a 0.2 μm filter system. After the incubation, the plate was decanted and the substrate was added and incubated for 30 minutes at room temperature. The plate was then decanted and left at room temperature to dry. Once dried the plate was read using a CTL S6 Universal-V Analyzer.

3.0 Results

3.1 Nanoparticle adjuvant matched the immunogenicity of the non-adjuvanted vaccine

A 28-day mouse study was conducted on 90 female ICR mice, 4-6 weeks old. The mice were grouped into three groups: placebo group (n=10), non-adjuvanted vaccine (n=40), and nanoparticle-adjuvanted vaccine (n=40). The two vaccine groups were then subdivided into four dosage groups, 10 mice in each dose group. On Day 28 all the mice in the study were exsanguinated and their blood was processed to sera. Once the sera was ready for testing it was heat-inactivated. In order to determine if the vaccine would be able to create neutralizing antibodies a micro-neutralization assay was performed on the serum from the mouse study. On the day of testing, the sera sample were plated and titrated up and the diluted virus was added. After a two-hour incubation, where any neutralizing antibodies were allowed to clear the virus, the virus/serum mixture was transferred to 96-well plates that had been seeded with Vero WHO cells. The plates were

then placed in an incubator over night and the following day were developed and read at 620 nm.

The OD data was used to generate geometric mean titers (GMTs) for each vaccine dilution tested and analyzed by Prism's 4-parameter logistics non-linear regression model to determine a median immunizing dose (ID50%). All mice the in the study were grouped into four dosage groups. For the non-adjuvanted CHIK PIV: 1400 ng (n=10), 280 ng (n=10), 56 ng (n=10), and 11.2 ng (n=10). For the nanoparticle-adjuvanted CHIK PIV: 1200 ng (n=10), 240 ng (n=10), 48 ng (n=10), and 9.6 ng (n=10). Neutralizing antibodies were detected in all does groups for the non-adjuvanted CHIK PIV vaccine and were detected in all groups but the lowest dosage group for the nanoparticle-adjuvanted vaccine. The geometric mean titers for the non-adjuvanted vaccine were: 418 in the 1400 ng group, 103 in the 280 ng group, <10 (9) in the 56 ng group, and 12 in the 11.2 ng group (**Figure 7**). For the nanoparticle-adjuvanted vaccine the geometric mean titers were: 428 in the 1200 ng group, 39 in the 240 ng group, <10 (8) in the 48 ng group, and <10 (5) in the 9.6 ng group (**Figure 7**). Though the nanoparticle-adjuvanted CHIK PIV vaccine had an initial slightly lower antigen concentration compared to the non-adjuvanted vaccine, there was no real difference between the GMTs.

The ID50% for the nanoparticle-adjuvanted vaccine was 107 and the ID50% for the non-adjuvanted vaccine was 81. Even though the neutralizing titer was higher for the nanoparticle-adjuvanted vaccine, the dose needed to elicit neutralization in 50% of patients was lower for the non-adjuvanted vaccine. It is difficult to compare the GMTs

and ID50%_s since the dosage concentrations were not the same but there still was not any substantial difference between the two.

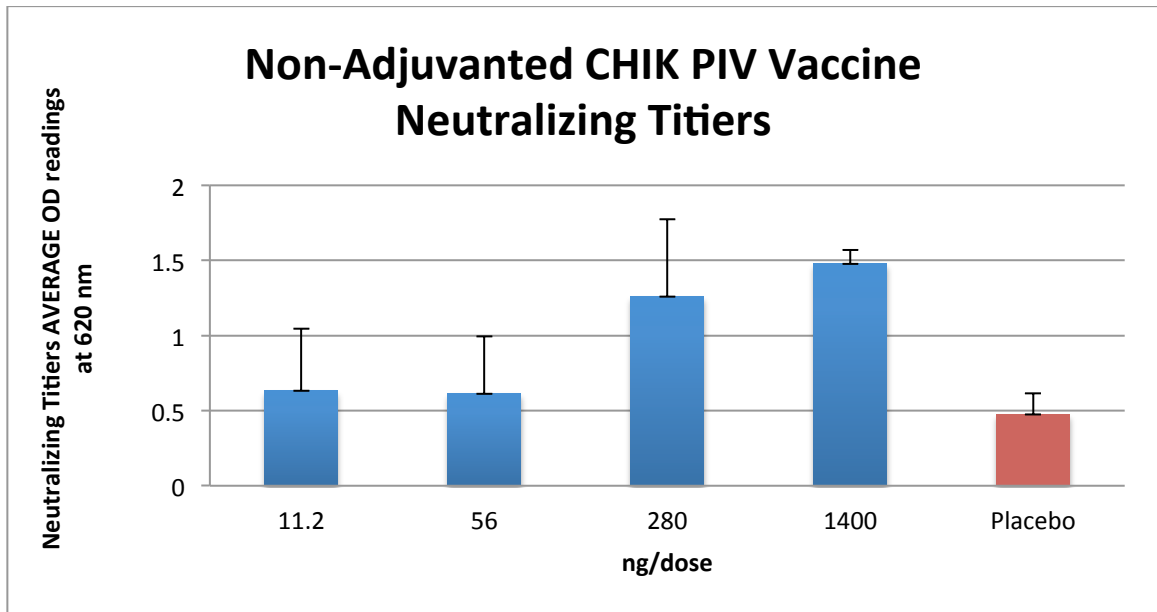
A

CHIKV PIV (14µg/ml)—NON-Adjuvant			
ng/Dose	SeroPositive Rate		GMT
	PIV Dilution	CHIKV	
1400	1:2	10/10 or 100%	418
280	1:10	8/10 or 80%	103
56	1:50	2/10 or 20%	<10 (9)
11.2	1:250	4/10 or 40%	12
Mouse ID50		81	
Mouse ID50 (95% C.I.)		34-192	

B

CHIKV PIV (12µg/ml)--in Nanoparticles			
ng/Dose	SeroPositive Rate		GMT
	PIV Dilution	CHIKV	
1200	1:2	10/10 or 100%	428
240	1:10	8/10 or 80%	39
48	1:50	2/10 or 20%	<10 (8)
9.6	1:250	0/10 or 0%	<10 (5)
Mouse ID50		107	
Mouse ID50 (95% C.I.)		103-111	

C.



D.

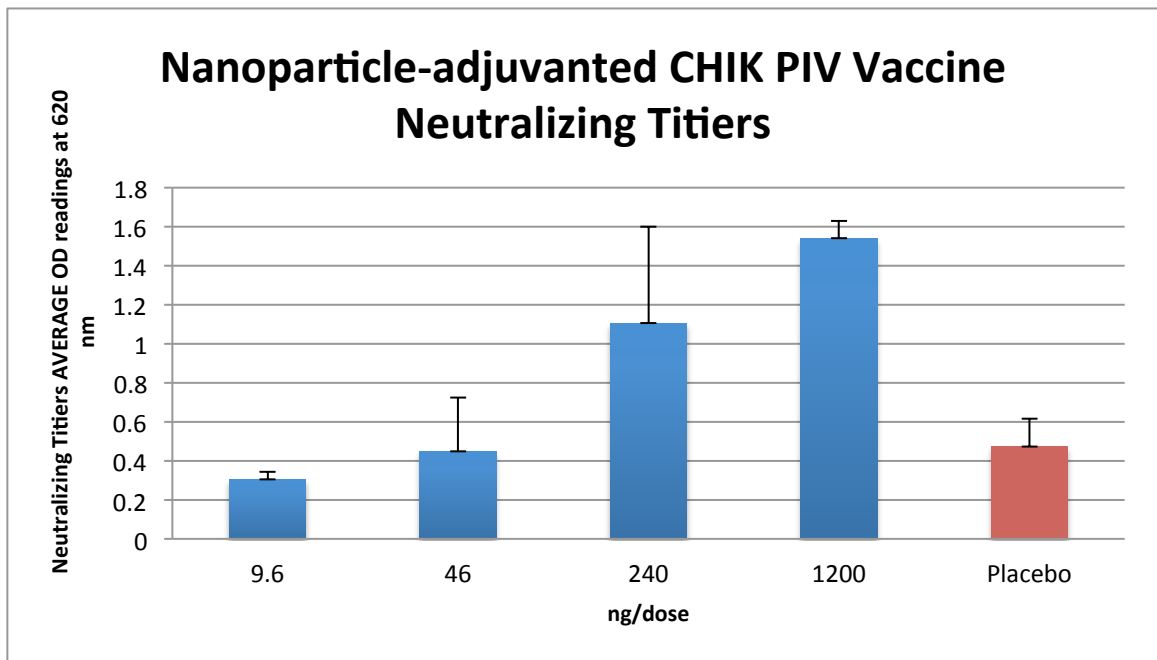


Figure 7. Neutralizing geometric mean titers and Seropositive Rate for neutralization.

All mice were grouped into four dosage groups. For the non-adjuvanted CHIK PIV: 1400 ng (n=10), 280 ng (n=10), 56 ng (n=10), and 11.2 ng (n=10). For the nanoparticle-adjuvanted CHIK PIV: 1200 ng (n=10), 240 ng (n=10), 48 ng (n=10), and 9.6 ng (n=10).

A) The GMTs for each dose of antigen for the non-adjuvanted CHIKV PIV and the seropositive rate for neutralization. Neutralizing antibodies were detected in all dose groups for the non-adjuvanted CHIK PIV vaccine. The ID50% for the nanoparticle-adjuvanted vaccine was 107. B) The GMTs for each dose of antigen for the nanoparticle-adjuvanted CHIKV PIV and the seropositive rate for neutralization. Neutralizing antibodies were detected in all groups but the lowest dosage group for the nanoparticle-adjuvanted vaccine. The ID50% for the non-adjuvanted vaccine was 81. C and D) show the average OD values for each dosage group in the non-adjuvanted CHIKV PIV group and in the nanoparticle adjuvanted group. The red column represents the placebo mouse group. The non-adjuvanted CHIKV PIV group had slightly higher OD values, indicating it had more neutralization in each dosage group.

3.2 Determine the cell-mediated immunity from the mouse spleens.

Once the mice had been exsanguinated, their spleens were removed, placed in a solution of DMEM, 10% DMSO, 10% FBS, and 1% gentamicin and then placed in Mr. Freezy for a slow freeze. When the spleens were ready to be processed they were placed in a 36.9 °C water bath until the cryopreservation liquid was thawed. The spleens were

placed in a cell strainer, mashed and washed. The cell suspension was spun several times to wash the cells. Once the cell suspension was ready it was counted to determine the number of viable cells.

A spleen from the non-adjuvanted group and a spleen from the placebo group were used for the first attempt to retrieve viable cells from the frozen spleens. The total cells recovered from the placebo group spleen was 2.57×10^5 and the total cells recovered from the non-adjuvanted group spleen was 3.22×10^5 . 2×10^4 per well was plated for the placebo spleen and 3×10^4 per well was plated for the non-adjuvanted spleen. The wells were stimulated with the CHIK PIV antigen overnight and the following day the plate was developed. The first trial showed no development of spots.

A second attempt to recover viable cells was conducted using a spleen from the non-adjuvanted group and from the NP-adjuvanted group. The same procedure was used to extract cells from the spleens but there was less time between when the spleens spent thawed and when they were mashed. When the second group of splenocytes were ready for counting they had similarly low count, 1×10^6 total cells. Due the low cell count the second ELISpot could not be done.

4.0 Discussion

In the 28-day mouse study two groups of female ICR mice, 40 mice per group, were tested with a non-adjuvanted CHIK PIV vaccine and a nanoparticle-adjuvant CHIK PIV vaccine. Each vaccine group was divided into 4 dosage groups comprising of ten mice each. The non-adjuvanted vaccine dosage groups were 1400 ng, 280 ng, 56 ng, and 11.2 ng. The nanoparticle-adjuvanted vaccine dosage groups were 1200 ng, 240 ng, 48

ng, and 9.6 ng. Based on the molecular weight of E1, E2, and C protein and the three dimensional structure of the chikungunya virus resolved with CryoEM the estimated molecular weight of one chikungunya virus particle is 36 M Da³⁸. This results in a weight of 60 actograms per viral particle. The highest vaccine dose contained 1400 ng/mL which results in 11 log₁₀ viral particle/mL or 1.1 log₁₀ viral particle in a 0.2 mL dose (the volume that was administrated to all the mice in the 1400 ng/mL dose group). This is consistent with vaccine preparations used for other alphaviruses including Dengue (16 log₁₀ copy number as quantified via qRT-PCR)³⁹. Each group was given their respected dose on Day 0 and then received a booster shot of the same dose on Day 14. On Day 28 all the mice we exsanguinated, their blood processed to sera and their spleens removed and cryopreserved. Results from the micro-neutralizing antibody assay, **Figure 7**, showed that the non-adjuvanted CHIK PIV vaccine had similar geometric mean titers of neutralizing antibodies to the nanoparticle-adjuvanted CHIK PIV vaccine. The GMT was higher for the nanoparticle-adjuvanted vaccine at the 1200 ng/dose compared to the non-adjuvanted vaccine. For the other dosage groups the non-adjuvanted had a slightly higher GMT, but this comparison is not completely accurate since the non-adjuvanted vaccine had slightly higher antigen concentrations than the nanoparticle-adjuvant vaccine for each dose group. The ID₅₀ was lower for the non-adjuvanted vaccine, 81, compared to the nanoparticle-adjuvanted vaccine, 107.

Neutralizing antibodies are a good measure for a vaccine's ability to protect against the virus but it is not necessarily the only means of measuring the immunogenicity of a vaccine. Looking at memory B cells and the level of T cells

produced is also important. Unfortunately, not enough viable cells were able to be cultured from the mouse spleens in this study to determine the level of Th1 cells and Th2 cells. There also was not enough CHIKV antigen and viable spleen cells to come up with an assay to determine the level of memory B cells. One reason for the inability to recover splenocytes from the mice could have been from the way the spleens were frozen. After the spleens were removed from the mice they were placed in a solution of DMEM, 10% DMSO, 10% FBS, and 1% gentamicin and then slowly frozen. When the spleens were placed in the freezing solution it might not have had enough time to penetrate the tissue completely, allowing the solution to protect the cells from death during the freezing process. Any other reason for the poor splenocyte recovery could be the fact that spleens cannot be frozen if recovering healthy cells is the goal.

Going forward, the next step for determining the efficacy of the vaccine candidate would be to conduct a non-human primate challenge study. A challenge study would be able to show the exposure-response. The nanoparticles could be taking the vaccine a different route than the non-adjuvanted vaccine is going and could produce more effective antibodies for clearing the virus and long lasting memory compared to the non-adjuvanted vaccine. Another particle screening needs to be conducted using the same viral particle concentration that will be used in the challenge study. In the initial screen that was conducted prior to the mouse study each particle screened had a $5.5 \log_{10}$ viral particle concentration. This was a lot higher than the $1.1 \log_{10}$ viral concentration that was administered to the mice in the highest vaccine dose group of 1400 ng/mL. The difference in viral concentrations could have effects on the NP capture kinetics. Another

aspect to look for the potential use of NPs as an adjuvant would be to load the NPs with an alum-adjuvanted vaccine and to see if the NP enhances the immune response elicited by an alum-adjuvanted CHKV vaccine.

CHAPTER FOUR: DETERMINATION OF THE LEVEL OF TOXICITY OF THE HYDROGEL NANOTRAP NANOPARTICLES IN MOUSE MODEL

For a vaccine to continue onto clinical trials it must show no sign of toxicity in any animal model. The vaccine alone or any added component, such as an adjuvant, cannot show any harm to the animals in initial trials or else it is not able to continue onto human trials.

1.0 Introduction

Vaccine development is a long, complex process, often lasting 10-15 years and involving a combination of public and private involvement. At the end of the 19th century, several vaccines for humans had been developed. However, no regulation of vaccine production existed. On July 1, 1902, the U.S. Congress passed "An act to regulate the sale of viruses, serums, toxins, and analogous products," later referred to as the Biologics Control Act. This was the first modern federal legislation to control the quality of drugs. This act emerged in part as a response to 1901 contamination events in St. Louis and Camden involving smallpox vaccine and diphtheria antitoxin⁴⁰. The Act created the Hygienic Laboratory of the U.S. Public Health Service to oversee manufacture of biological drugs. The Hygienic Laboratory eventually became the National Institutes of Health. The Act established the government's right to control the establishments where vaccines were made⁴⁰.

The United States Public Service Act of 1944 mandated that the federal government issued licenses for biological products, including vaccines⁴⁰. In the United States, vaccine development and testing follow a standard set of steps. Regulation and oversight increase as the candidate vaccine makes its way through the process. The first stage is the exploratory stage⁴⁰. This stage involves basic laboratory research and often lasts 2-4 years. Federally funded academic and governmental scientists identify natural or synthetic antigens that might help prevent or treat a disease. These antigens could include virus-like particles, weakened viruses or bacteria, weakened bacterial toxins, or other substances derived from pathogens. The second step is the pre-clinical stage. Pre-clinical studies use tissue-culture or cell-culture systems and animal testing to assess the safety of the candidate vaccine and its immunogenicity, or ability to provoke an immune response⁴⁰. Animal subjects may include mice and monkeys. These studies give researchers an idea of the cellular responses they might expect in humans. They may also suggest a safe starting dose for the next phase of research as well as a safe method of administering the vaccine. They may also do challenge studies with the animals. These preliminary steps are crucial for a vaccine to move onto the next stages of vaccine development and approval. If the vaccine shows to be toxic or does not produce the desired immune responses the vaccine candidate will fail and not progress beyond this point.

Animal models can be used in a variety of ways to study disease pathogenesis, host–pathogen interactions and mechanisms of protection following vaccination, infection or treatment of disease. Animal models can also serve to analyze specific

aspects of the immune response, such as the development of immune organs, the role of specific immune compartments or individual cell populations, the trafficking of immune cells following infection or vaccination, as well as various aspects of vaccine delivery including mucosal or topical application¹⁵. The development of effective vaccines also requires proper vaccine formulation and delivery, which is critical to achieve immune-mediated protection against infection. Animal models have been used to explore various aspects of vaccine formulation and delivery, including the route of administration, targeting to specific receptors and the induction of mucosal versus systemic immunity¹⁵. Furthermore, when evaluating vaccine safety and possible side effects to immunization, the use of appropriate animal models is critical.

Toxicity has been a major issue for the nanoparticle field of study. NPs have been prepared from metal and non-metal, polymeric materials and bioceramics. Even though humans are exposed to various nano-scale materials throughout their lives, the new emerging field of nanotechnology has become another threat to human life. Because of their small size, NPs find their way easily to enter the human body and cross the various biological barriers and may reach the most sensitive organs⁴¹. Scientists have proposed that NPs of size less than 10 nm act similar to a gas and can enter human tissues easily and may disrupt the cell normal biochemical environment⁴¹. NPs are more toxic to human health in comparison to large-sized particles of the same chemical substance, and it is suggested that toxicities are inversely proportional to the size of the NPs⁴¹.

Studies have reported that aluminum-based NPs disturb the cell viability, alter mitochondrial function, increase oxidative stress, genotoxic effect, and also alter tight

junction protein expression of the blood brain barrier (BBB)^{41–43}. Other studies have shown the toxicity from aluminum-based NPs is based on size of the particle and/or dose-dependent⁴⁴. Gold NPs have for the most part shown to be non-toxic. However, there are some other reports suggesting that cytotoxicity associated with gold NPs depends on dose, side chain (cationic) and the stabilizer used^{41,45–47}. Historically, silver has been known for its anti-bacterial properties and its NPs have been used for a wide range of applications^{41,48}. But some studies have reported that silver NPs can have varying degrees of cytotoxicity depending on the different coatings^{41,49}. Iron oxide is another NP that has been used in biomedical, drug delivery, and diagnostic fields. But studies have shown these NPs are able to bioaccumulate in the liver and other reticuloendothelial system organs^{41,50,51}. *In vivo* studies have shown that after entering the cells, iron oxide NPs remain in cell organelles (endosomes/lysosomes), release into cytoplasm after decomposing, and contribute to cellular iron pool⁴¹. Magnetic iron oxide NPs have been observed to accumulate in the liver, spleen, lungs, and brain after inhalation, showing its ability to cross BBB^{41,52}. Evidence show that these NPs exert their toxic effect in the form of cell lysis, inflammation, and disturbing blood coagulation system^{41,53}.

The carbon-based nanomaterials, such as carbon nanotubes, fullerenes, single and multi-walled carbon nanotubes are the most attractive and are widely used nanomaterials⁴¹. Carbon-based nanomaterials have been reported in literature as cytotoxic agents. Some studies have reported that their cytotoxicity is size-dependent^{41,54,55}. Along with size-dependent toxicity, carbon-based NP's method of preparation and the presence of trace metals determine the extent of toxicity and biological response of the cells^{41,56,57}.

In this study, the toxicity induced by subcutaneous injections of Nanotrap nanoparticles in mice was tested.

2.0 Methods

2.1: Toxicity examination on mice used in study

Post exsanguination an initial visual examination for toxicity was performed on five mice from each vaccine group. Each mouse was weighed and their tails, whiskers and fur were examined for any signs of distress or sickness. Next, a necropsy was performed on each mouse. The abdomen cavity was opened and the abdominal organs were examined for gross signs of toxicity. A small section of the heart, lungs, spleen, liver, and kidneys were taken and fixed with formalin. The tissue samples were then sent out to AML Laboratories. There they were embedded in paraffin wax blocks, and sliced to about 5 μm and placed on the glass slide. The cross-sections were stained with H&E. Each slide was examined under a light microscope for any discernible signs of toxicity.

3.0 Results

3.1: No signs of toxicity.

Each mouse was weighed and their tails, whiskers and fur were examined for signs of toxicity (**Table 1**). All mice had similar weights when compared to the placebo mice and all the mice had healthy, well-groomed fur without any superficial lesions. The mice also had healthy, long whiskers. A few of the mice appeared to have trace amounts of blood around their nose. Once the mice were opened, their organs were examined. All

organs appear to be glistening and showed no discoloration, tumors or necrosis. The intestines had digested food, indicating the mice had been eating during the 28-day study. The skin at the sight of injection was also examined and showed signs of inflammation.

Table 1. Initial mouse toxicity examination. All mice were weighed, externally examined for signs of toxicity and necropsied for an internal examination of toxicity. The average weight for the mice in the placebo group was 29.95 g. The average weight for the non-adjuvanted group was 33.67 g and the average for the nanoparticle-adjuvant group was 25.69 g. There was no significant difference in weight between the groups, $p=0.2$. Their whiskers and tails looked healthy and their fur appeared groomed. Once the mice had been necropsied their internal organs were examined for signs of toxicity. All organs looked healthy and had no signs of discoloration, tumors, or necrosis.

ID	Weight (g)	Appearance of fur	Appearance of whisker	Appearance of nose	Appearance of gross anatomy
Placebo #6	25.26	Healthy	Healthy	Healthy	Healthy
Placebo #7	28.55	Healthy	Healthy	Blood around nose	Healthy
Placebo #8	32.46	Healthy	Healthy	Healthy	Healthy
Placebo #9	31.90	Healthy	Healthy	Healthy	Healthy
Placebo #10	31.57	Healthy	Healthy	Healthy	Healthy
Non-adjuvanted CHIK PIV #6	32.73	Healthy	Healthy	Healthy	Healthy
Non-adjuvanted CHIK PIV #7	31.93	Healthy	Healthy	Healthy	Healthy
Non-adjuvanted CHIK PIV #8	35.60	Healthy	Healthy	Healthy	Healthy
Non-adjuvanted CHIK PIV #9	29.24	Healthy	Healthy	Healthy	Healthy
Non-adjuvanted CHIK PIV #10	38.83	Healthy	Healthy	Healthy	Healthy

Nanoparticle- adjuvanted CHIK PIV #6	28.33	Healthy	Healthy	Healthy	Healthy
Nanoparticle- adjuvanted CHIK PIV #7	35.44	Healthy	Healthy	Blood around nose	Healthy
Nanoparticle- adjuvanted CHIK PIV #8	30.99	Healthy	Healthy	Healthy	Healthy
Nanoparticle- adjuvanted CHIK PIV #9	29.70	Healthy	Healthy	Healthy	Healthy
Nanoparticle- adjuvanted CHIK PIV #10	30.98	Healthy	Healthy	Healthy	Healthy

H&E stained slides from the placebo group, non-adjuvanted vaccine group and the nanoparticle vaccine group were examined under a light microscope. Signs of toxicity in the cross-sections , such as inflammatory cells or dead cells would appear black and clumped together. In the liver, changes in the nuclei, the appearance of fat cells or fibrosis would be considered signs of toxicity. In the spleen, toxicity generally would appear dark and in whole regions. Signs of toxicity in the heart would be fibrosis. All the slides were examined for signs of toxicity. The hearts, lunges, kidneys, spleens and livers for the placebos, non-adjuvanted vaccine group and NP-adjuvanted vaccine group were all healthy and had no signs of inflammation or cell death. In the kidneys, the glomeruli looked healthy and the tubules showed no sign of inflammatory cells. The livers also showed no signs of inflammatory cells, fatty lipid changes and the hepatocyte nuclei all looked similar and without abnormality. There were also no signs of fatty infiltration or fibrosis in the liver and no signs of fibrosis in the heart. For the most part the lungs looked healthy, except for the presences of fluid in the alveoli. There was a presence of

fluid in the lung of all mice (placebo, non adjuvanted and adjuvanted). Overall, there were no discernible signs of toxicity in the placebo group, or non-adjuvanted vaccine group or the NP-adjuvanted vaccine group.

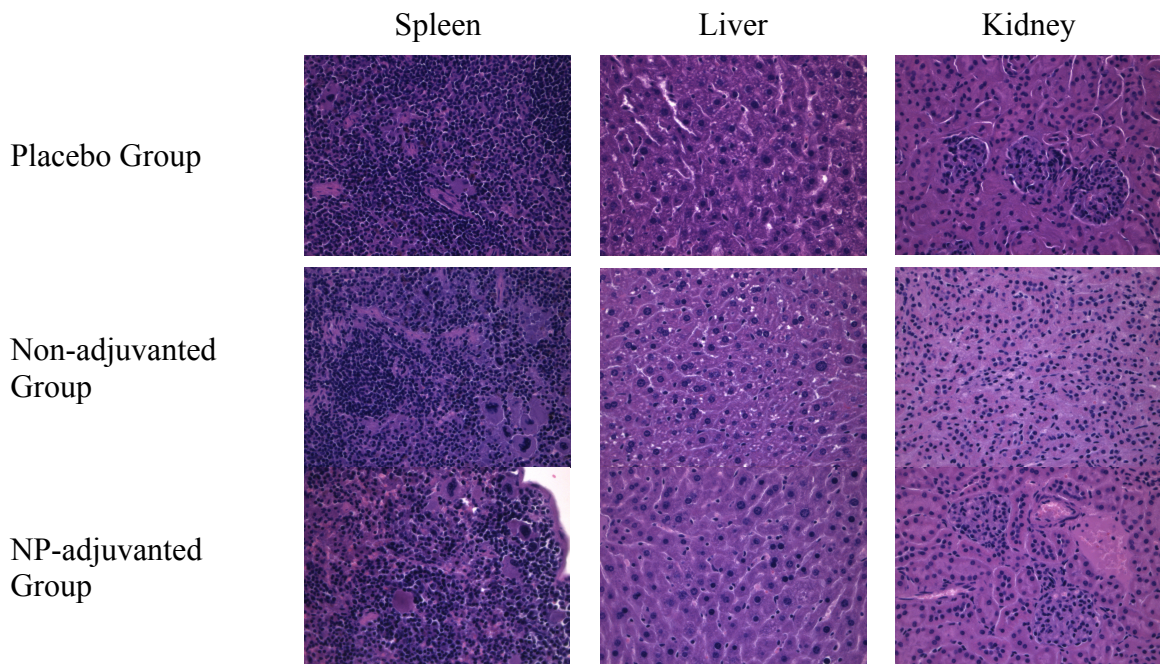


Figure 8. Tissue toxicity examination. Tissue samples of all major organs in each mouse were taken, fixed in formalin, embedded in paraffin wax blocks, and sliced to about 5 μm and placed on the glass slide. The cross-sections were stained with H&E. All cross-sections appeared to have no signs of toxicity. There were no signs of dead cells or inflammatory cells.

4.0 Discussion

Nanoparticles are used in a wide range of areas and their use will only increase. Human exposure to NPs is inevitable, whether it be intentionally or unintentionally. Before they can be considered for human application, such as medical application, all NPs must be subject to toxicology studies.

To determine the level of toxicity for the CHIK PIV vaccine mice from the 28-day long mouse trial were visually examined and weighed post exsanguination and examined internally. For visual signs of toxicity the mice whiskers, fur coats and noses were examined. Healthy mice continue to groom their coats, their whiskers appear long and healthy and their noses are pink and have no abnormalities. Gross signs of toxicity in the liver would be pale areas and areas of necrosis and embolisms. Other gross signs of toxicity would be a lack of digested food in the intestines, indicating the mice have stopped eating, and the organs no longer glistening and show discoloration or necrosis. Five mice from each vaccine group were selected for a post-exsanguination examination and necropsy. All mice were first weighed. The average weight for the placebo group was 29.95 g. The average weight for the non-adjuvanted group was 33.67 g and the average for the nanoparticle-adjuvant group was 25.69 g. There was no statistical ($p=0.2$) difference in weight between the groups, showing that all the mice were eating normally.

All mice also appeared to have groomed, healthy looking fur and long whiskers. When the health of the mice begins to decline the mice stop grooming themselves but there was no sign the mice were no longer healthy enough to care for themselves.

Discoloration in the nose is another visual sign the health of the mouse is declining from toxicity; anything other than a pink nose could be an indication of illness. All but two of the mice, #7 mouse from the placebo group and #7 mouse from the nanoparticle group, had healthy pink noses. Mouse #7 from both the placebo and nanoparticle group had trace blood around their noses, which was most likely was from the exsanguination process. When skin is penetrated or cut neutrophils, microphages and other proteins and fluids migrate to the sight of injection. The cellular activity and leaky blood vessels can cause swelling and a foreign body reaction may be generates at the sight on injection. Any initial reaction or cellular response to the vaccine would first appear in the skin around the injection sight, such as inflammation and redness of skin. The lose skin on the back, the sight of injection, was examined for any signs of inflammation. None of the mice showed any signs of local redness or swelling at the site of injection, indicating there was no reaction to the injected substance.

After the visual inspection all the mice were necropsied. Their internal organs were visually examined for signs of toxicity. All mice had no signs of necrosis on their organs. The organs all looked healthy and were glossy. The mice's intestines also had digested food, indicating they were eating normally during the study. A lack of food in the intestines could mean that the mice have lost their appetite, a sign that their health is declining.

Once the internal organs of all the mice were examined, small samples were taken of all the major organs and placed in formalin. The tissue samples of the lunges, heart, spleen, kidney, and liver were sent out to be fixed to slides and stained. All the slides

from each vaccine group were examined for signs of toxicity. Cellular signs of toxicity in the liver might be swollen cells, increased levels of fat cells or fibrosis, changes in the nuclei, or clumps of dead cells or white blood cells. The blood filters through the liver, removing any toxins, making it the most sensitive organ to toxins. When the liver starts to show signs of toxicity two things will happen to the liver; lipogenesis, which is formation of fat cells, and fibrosis, the formation of excess fibrous connective tissue. All the liver cross-sections showed no signs of fat cells, fibrosis or inflammation, they all looked healthy.

The spleen is another organ that filters toxins out of the blood. Both the liver and spleen are the primary organs to examine when looking for toxicity. Normally in the spleen, if there are signs of toxicity it will happen in whole regions and appear dark. There are also macrophages present in the peripheral of the spleen and if there is toxicity they tend to move towards the center. The cross-sections of the spleens from the placebo group, non-adjuvanted group and NP-adjuvanted group looked healthy and had no regions of toxicity.

The kidneys filter toxins from the blood and excrete them through the urine. If toxins are found in the kidneys, white blood cells and inflammation cells would be present in their cross-sections. When the kidney cross-sections were examined there was no sign of white blood cells in the tubules.

The heart cross-sections were also examined under a microscope and all appeared healthy and had no signs of fibrosis, a sign there is damage or toxicity to the organ. The lungs were also examined and appeared to be healthy except for the fact there was fluid

in the alveoli. This did not cause alarm since the placebo mice lung cross-sections had fluid in their alveoli, suggesting that it was related to the method of euthanasia since it is common for fluid to fill the lungs at death. Overall, there were no signs of discernible toxicity in any of the mice. Going forward, the next step will be to conduct a formal toxicity study, where the mice are given increasingly higher doses of NPs to determine if any toxicity is created with the NPs.

REFERENCES

1. Powers, A. M. *et al.* Evolutionary Relationships and Systematics of the Alphaviruses. *J. Virol.* **75**, 10118–10131 (2001).
2. Tiwari, M. *et al.* Assessment of immunogenic potential of Vero adapted formalin inactivated vaccine derived from novel ECSA genotype of Chikungunya virus. *Vaccine* **27**, 2513–2522 (2009).
3. Pulmanausahakul, R., Roytrakul, S., Auewarakul, P. & Smith, D. R. Chikungunya in Southeast Asia: understanding the emergence and finding solutions. *Int. J. Infect. Dis. IJID Off. Publ. Int. Soc. Infect. Dis.* **15**, e671-676 (2011).
4. Sourisseau, M. *et al.* Characterization of Reemerging Chikungunya Virus. *PLOS Pathog* **3**, e89 (2007).
5. Schwartz, O. & Albert, M. L. Biology and pathogenesis of chikungunya virus. *Nat. Rev. Microbiol.* **8**, 491–500 (2010).
6. Solignat, M., Gay, B., Higgs, S., Briant, L. & Devaux, C. Replication cycle of chikungunya: a re-emerging arbovirus. *Virology* **393**, 183–197 (2009).
7. Ng, L. C. & Hapuarachchi, H. C. Tracing the path of Chikungunya virus--evolution and adaptation. *Infect. Genet. Evol. J. Mol. Epidemiol. Evol. Genet. Infect. Dis.* **10**, 876–885 (2010).

8. Long, K. M. & Heise, M. T. Protective and Pathogenic Responses to Chikungunya Virus Infection. *Curr. Trop. Med. Rep.* **2**, 13–21 (2015).
9. Krejbich-Trotot, P. *et al.* Chikungunya virus mobilizes the apoptotic machinery to invade host cell defenses. *FASEB J. Off. Publ. Fed. Am. Soc. Exp. Biol.* **25**, 314–325 (2011).
10. Gutjahr, A. *et al.* Biodegradable Polymeric Nanoparticles-Based Vaccine Adjuvants for Lymph Nodes Targeting. *Vaccines* **4**, 34 (2016).
11. Borgherini, G. *et al.* Outbreak of Chikungunya on Reunion Island: Early Clinical and Laboratory Features in 157 Adult Patients. *Clin. Infect. Dis.* **44**, 1401–1407 (2007).
12. Weaver, S. C., Osorio, J. E., Livengood, J. A., Chen, R. & Stinchcomb, D. T. Chikungunya virus and prospects for a vaccine. *Expert Rev. Vaccines* **11**, 1087–1101 (2012).
13. Powers, A. M. & Logue, C. H. Changing patterns of chikungunya virus: re-emergence of a zoonotic arbovirus. *J. Gen. Virol.* **88**, 2363–2377 (2007).
14. Morens, D. M. & Fauci, A. S. Chikungunya at the Door — Déjà Vu All Over Again? *N. Engl. J. Med.* **371**, 885–887 (2014).
15. Gerdt, V., Littel-van den Hurk, S. van D., Griebel, P. J. & Babiuk, L. A. Use of animal models in the development of human vaccines. *Future Microbiol.* **2**, 667–675 (2007).

16. Tsetsarkin, K. A., Vanlandingham, D. L., McGee, C. E. & Higgs, S. A Single Mutation in Chikungunya Virus Affects Vector Specificity and Epidemic Potential. *PLOS Pathog* **3**, e201 (2007).
17. Gorchakov, R. *et al.* Attenuation of Chikungunya virus vaccine strain 181/clone 25 is determined by two amino acid substitutions in the E2 envelope glycoprotein. *J. Virol.* **86**, 6084–6096 (2012).
18. Chang, L.-J. *et al.* Safety and tolerability of chikungunya virus-like particle vaccine in healthy adults: a phase 1 dose-escalation trial. *The Lancet* **384**, 2046–2052 (2014).
19. Jordan Report 2012. *Scribd* Available at: <https://www.scribd.com/document/314842062/Jordan-Report-2012>. (Accessed: 27th October 2016)
20. Reed, S. G., Bertholet, S., Coler, R. N. & Friede, M. New horizons in adjuvants for vaccine development. *Trends Immunol.* **30**, 23–32 (2009).
21. Exley, C., Siesjö, P. & Eriksson, H. The immunobiology of aluminium adjuvants: how do they really work? *Trends Immunol.* **31**, 103–109 (2010).
22. Brewer, J. M. (How) do aluminium adjuvants work? *Immunol. Lett.* **102**, 10–15 (2006).
23. Kool, M., Fierens, K. & Lambrecht, B. N. Alum adjuvant: some of the tricks of the oldest adjuvant. *J. Med. Microbiol.* **61**, 927–934 (2012).
24. Sahdev, P., Ochyl, L. J. & Moon, J. J. Biomaterials for nanoparticle vaccine delivery systems. *Pharm. Res.* **31**, 2563–2582 (2014).

25. Nicholls, E. F., Madera, L. & Hancock, R. E. W. Immunomodulators as adjuvants for vaccines and antimicrobial therapy. *Ann. N. Y. Acad. Sci.* **1213**, 46–61 (2010).
26. Smith, D. M., Simon, J. K. & Baker, J. R. Applications of nanotechnology for immunology. *Nat. Rev. Immunol.* **13**, 592–605 (2013).
27. Gregory, A. E., Titball, R. & Williamson, D. Vaccine delivery using nanoparticles. *Front. Cell. Infect. Microbiol.* **3**, 13 (2013).
28. Zhao, L. *et al.* Nanoparticle vaccines. *Vaccine* **32**, 327–337 (2014).
29. Popova, T. G. *et al.* Chemokine-Releasing Nanoparticles for Manipulation of Lymph Node Microenvironment. *Nanomater. Basel Switz.* **5**, 298–320 (2015).
30. Burt, F. J., Rolph, M. S., Rulli, N. E., Mahalingam, S. & Heise, M. T. Chikungunya: a re-emerging virus. *Lancet Lond. Engl.* **379**, 662–671 (2012).
31. Luchini, A. *et al.* Smart Hydrogel Particles: □ Biomarker Harvesting: □ One-Step Affinity Purification, Size Exclusion, and Protection against Degradation. *Nano Lett.* **8**, 350–361 (2008).
32. Luchini, A. *et al.* Nanoparticle technology: addressing the fundamental roadblocks to protein biomarker discovery. *Curr. Mol. Med.* **10**, 133–141 (2010).
33. Tamburro, D. *et al.* Multifunctional Core–Shell Nanoparticles: Discovery of Previously Invisible Biomarkers. *J. Am. Chem. Soc.* **133**, 19178–19188 (2011).
34. Shafagati, N. *et al.* The use of NanoTrap particles as a sample enrichment method to enhance the detection of Rift Valley Fever Virus. *PLoS Negl. Trop. Dis.* **7**, e2296 (2013).

35. Siegrist, C.-A. in *Vaccines (Sixth Edition)* (eds. Orenstein, W. A. & Offit, P. A.) 14–32 (W.B. Saunders, 2013).
36. Smalley, C., Erasmus, J. H., Chesson, C. B. & Beasley, D. W. C. Status of research and development of vaccines for chikungunya. *Vaccine* **34**, 2976–2981 (2016).
37. Poo, Y. S. *et al.* Multiple immune factors are involved in controlling acute and chronic chikungunya virus infection. *PLoS Negl. Trop. Dis.* **8**, e3354 (2014).
38. Sun, S. *et al.* Structural analyses at pseudo atomic resolution of Chikungunya virus and antibodies show mechanisms of neutralization. *eLife* **2**, e00435 (2013).
39. Mantel, N. *et al.* Standardized quantitative RT-PCR assays for quantitation of yellow fever and chimeric yellow fever–dengue vaccines. *J. Virol. Methods* **151**, 40–46 (2008).
40. Vaccine Development, Testing, and Regulation | History of Vaccines. Available at: <http://www.historyofvaccines.org/content/articles/vaccine-development-testing-and-regulation>. (Accessed: 28th October 2016)
41. Bahadar, H., Maqbool, F., Niaz, K. & Abdollahi, M. Toxicity of Nanoparticles and an Overview of Current Experimental Models. *Iran. Biomed. J.* **20**, 1–11 (2016).
42. Chen, L., Yokel, R. A., Hennig, B. & Toborek, M. Manufactured aluminum oxide nanoparticles decrease expression of tight junction proteins in brain vasculature. *J. Neuroimmune Pharmacol. Off. J. Soc. NeuroImmune Pharmacol.* **3**, 286–295 (2008).

43. Radziun, E. *et al.* Assessment of the cytotoxicity of aluminium oxide nanoparticles on selected mammalian cells. *Toxicol. Vitro Int. J. Publ. Assoc. BIBRA* **25**, 1694–1700 (2011).
44. Alshatwi, A. A. *et al.* Al₂O₃ nanoparticles induce mitochondria-mediated cell death and upregulate the expression of signaling genes in human mesenchymal stem cells. *J. Biochem. Mol. Toxicol.* **26**, 469–476 (2012).
45. Goodman, C. M., McCusker, C. D., Yilmaz, T. & Rotello, V. M. Toxicity of gold nanoparticles functionalized with cationic and anionic side chains. *Bioconjug. Chem.* **15**, 897–900 (2004).
46. Boisselier, E. & Astruc, D. Gold nanoparticles in nanomedicine: preparations, imaging, diagnostics, therapies and toxicity. *Chem. Soc. Rev.* **38**, 1759–1782 (2009).
47. Connor, E. E., Mwamuka, J., Gole, A., Murphy, C. J. & Wyatt, M. D. Gold nanoparticles are taken up by human cells but do not cause acute cytotoxicity. *Small Wein. Bergstr. Ger.* **1**, 325–327 (2005).
48. Chen, X. & Schluesener, H. J. Nanosilver: a nanoproduct in medical application. *Toxicol. Lett.* **176**, 1–12 (2008).
49. Foldbjerg, R., Dang, D. A. & Autrup, H. Cytotoxicity and genotoxicity of silver nanoparticles in the human lung cancer cell line, A549. *Arch. Toxicol.* **85**, 743–750 (2011).
50. Naqvi, S. *et al.* Concentration-dependent toxicity of iron oxide nanoparticles mediated by increased oxidative stress. *Int. J. Nanomedicine* **5**, 983–989 (2010).

51. Albukhaty, S., Naderi-Manesh, H. & Tiraihi, T. In vitro labeling of neural stem cells with poly-L-lysine coated super paramagnetic nanoparticles for green fluorescent protein transfection. *Iran. Biomed. J.* **17**, 71–76 (2013).
52. Liu, G., Gao, J., Ai, H. & Chen, X. Applications and potential toxicity of magnetic iron oxide nanoparticles. *Small Wein. Bergstr. Ger.* **9**, 1533–1545 (2013).
53. Zhu, M.-T. *et al.* Comparative study of pulmonary responses to nano- and submicron-sized ferric oxide in rats. *Toxicology* **247**, 102–111 (2008).
54. Magrez, A. *et al.* Cellular toxicity of carbon-based nanomaterials. *Nano Lett.* **6**, 1121–1125 (2006).
55. Herzog, E. *et al.* A new approach to the toxicity testing of carbon-based nanomaterials--the clonogenic assay. *Toxicol. Lett.* **174**, 49–60 (2007).
56. Pulskamp, K., Diabaté, S. & Krug, H. F. Carbon nanotubes show no sign of acute toxicity but induce intracellular reactive oxygen species in dependence on contaminants. *Toxicol. Lett.* **168**, 58–74 (2007).
57. Donaldson, K. *et al.* Carbon nanotubes: a review of their properties in relation to pulmonary toxicology and workplace safety. *Toxicol. Sci. Off. J. Soc. Toxicol.* **92**, 5–22 (2006).

BIOGRAPHY

Kassandra Jackson graduated from Paul the VI Catholic High School, Fairfax, Virginia, in 2007. She received her Bachelor of Science from George Mason University in 2011. She was employed as a teacher in Prince William County for three years and then was hired as a microbiologist at Walter Reed Army Institute of Research. After spending two years working there she left to move to Hawaii to be with her fiancé and to pursue her career in infectious tropical diseases there.